# Ligand Control in Co-Catalyzed Regio- and Enantioselective Hydroboration. Homoallyl Secondary Boronates via Uncommon 4,3-Hydroboration of 1,3-Dienes

Mahesh M. Parsutkar<sup>‡</sup>, Subhajit Bhunia<sup>‡</sup>, Mayukh Majumder, Remy F. Lalisse, Christopher M. Hadad\* and T. V. RajanBabu\*

Department of Chemistry and Biochemistry, The Ohio State University, 100 West 18th Avenue, Columbus, Ohio 43210, USA.

**Supporting Information** 

**ABSTRACT:** Enantiopure homoallylic boronate esters are versatile intermediates because the C–B bond in these compounds can be stereospecifically transformed into C–C, C–O and C–N bonds. Regio- and enantioselective synthesis of these precursors from 1,3-dienes has few precedents in the literature. We have identified reaction conditions and ligands for the synthesis of nearly enantiopure (er >97:3 to >99:1) homoallylic boronate esters via a rarely seen cobalt-catalyzed [4,3]-hydroboration of 1,3-dienes. Monosubstituted or 2,4-disubstituted linear dienes undergo highly efficient, regio- and enantioselective hydroboration with HBPin catalyzed by  $[(L^*)Co]^{\dagger}[BARF]^{\dagger}$ , where L\* is typically a chiral bis-phosphine ligand with a narrow bite angle. Several such ligands (examples: *i*-PrDuPhos, QuinoxP\*, Duanphos and, BenzP\*) that give high enantioselectivities for the [4,3]-hydroboration product have been identified. In addition, the equally challenging problem of regioselectivity is uniquely solved with a dibenzooxaphosphole ligand, (*R*, *R*)-MeO-BIBOP. A cationic cobalt(I) complex of this ligand is a very efficient (TON >960) catalyst, while providing excellent regioselectivities (rr >98:2) and enantioselectivities (er >98:2) for a broad range of substrates. A detailed computational investigation of the reactions using Co-complexes from two widely different ligands (BenzP\* and MeO-BIBOP) employing B3LYP-D3 density functional theory provides key insights into the mechanism and the origins of selectivities. The computational results are in full agreement with the experiments. For the complexes we have examined thus far, the relative stabilities of the diastereomeric diene-bound complexes  $[(L^*)Co(\eta^4\text{-diene})]^+$  leads to the initial diastereofacial selectivity, which in turn is retained in the subsequent steps, providing exceptional enantioselectivity for the reactions.

### INTRODUCTION

Enantioenriched α-stereogenic organoboranes are versatile intermediates in organic synthesis because the C-B bonds can be stereospecifically converted into to C-C, C-O, and C-N bonds (Figure 1 A). Development of efficient, enantioselective methods for the synthesis of this class of compounds has received enormous attention.2 One of the most versatile and selective processes for the synthesis of chiral organoboranes is through enantioselective hydroboration of olefins. Enantioselective hydroborations of simple and activated alkenes including vinylarenes are well established.3 In sharp contrast, the catalytic regio- and enantioselective hydroborations of conjugated 1,3-dienes still remain an underdeveloped research area, mostly because of the formidable challenges involved in managing the regioselectivity, as a myriad of outcomes are possible even for a simple hydrofunctionalization reaction as shown in Figure 1 **B**.<sup>4</sup> Multiple HBPin additions could be another detraction. If successful, regio- and stereoselective hydroboration of 1,3dienes would provide a variety of homoallylic (1,2/4,3-additions) or allylic [2,1]/[3,4]/[1,4]/[4,1]-additions) boronates all of which are highly valuable synthons as the latent functional groups can be elaborated further.<sup>5</sup> Since secondary homoallylic boronates among these adducts can be stereospecifically

oxidized to homoallylic alcohols, this catalytic approach will be complementary to other catalytic procedures<sup>6a-d</sup> and the classical Brown's stoichiometric allylation of aldehydes and its variations.<sup>6e-h</sup> These reactions have found numerous applications in the synthesis of bioactive molecules.<sup>7</sup>

In transition metal-catalyzed hydroboration of acyclic 1,3dienes, there are many examples of the 'anti-Markovnikov' additions where boron adds to the least hindered C1-carbon of a 1,3-diene either in a [1,2]- or a [1,4]-manner,8 even though enantioselective variations of these reactions in prochiral acyclic dienes have been rare.9 To this end, our group disclosed a cobalt-catalyzed [1,2]-hydroboration of prochiral 1,3-dienes with HBPin employing chiral phosphinooxazoline complexes of low-valent cobalt (Figure 1 **D**). 10 However, the addition of boron at the more sterically hindered, C<sub>4</sub> position (i.e., to give [4,3]-or [4,1]-hydroboration) with high enantioselectivity remained an unmet challenge; moreover, this process from readily available 1,3-dienes would be complementary to some of the procedures listed earlier (see, for example Ref 2) for the synthesis of functionalized chiral homoallyl boronates. The first achiral regioselective Markovnikov addition of a boronate ester at the more sterically hindered C<sub>4</sub>-position of 4-substituted 1,3dienes was reported by Huang et al. (Figure 1 C). 11 However, this method required aryl substituents at the 4-postion for high regioselectivity, and simple alkyl-substituted linear 1,3-dienes lead to poor regioselectivity with [1,4]-adducts formed as the major product. Recently, while our manuscript was in preparation, <sup>12</sup> Diver et al. reported <sup>13</sup> [4,3]-hydroborations of 2,4-disubstituted 1,3-dienes, using chiral ligands in a Cu-catalyzed

aza-Matteson

Coupling partner

protoborylation. This reaction gave good regioselectivities (ranging from 3:1 to 20:1), but modest enantioselectivities (er of 83:17 to 93:7) (Figure 1 **D**). This protocol is also limited to 2,4-disubstituted 1,3-dienes.

# A. Stereospecific transformation of C-B bonds to C-C, C-N, C-O bonds Carbonyl allylation via homoallylic boronates Stoichiometric allylation methods Brown, Hoffmann, Roush, Leighton Versatile chiral precursor Versatile chiral precursor Carbonyl allylation via homoallylic boronates Stoichiometric allylation methods Brown, Hoffmann, Roush, Leighton Catalytic allylation methods Keck, Denmark, Krische

### B. Regioselectivity challenges in hydrofunctionalization of 1,3-dienes (convention used in this paper)

$$R^{2} = R^{3} = H$$

$$R^{2} = R^{3} = H$$

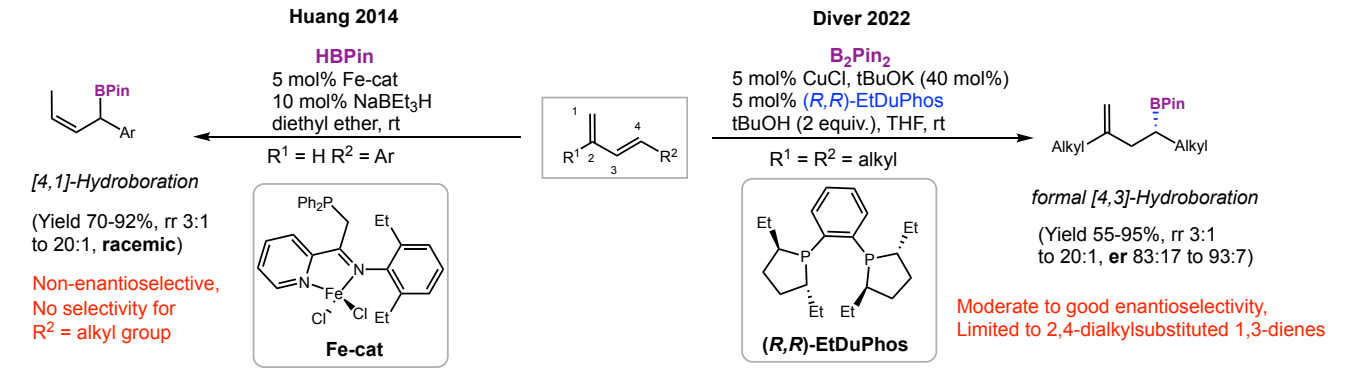
$$R^{3} = R^{2} = R^{3} = H$$

$$R^{4} = R^{2} = R^{3} = H$$

$$R^{4} = R^{2} = R^{3} = H$$

$$R^{4} = R^{4} = R^{4} + R^{4} +$$

### C. Fe- and Cu-catalyzed regioselective [4,1]- and [4,3]-hydroboration of 1,3-dienes



### D. Ligand controlled Co-catalyzed regiodivergent enantioselective hydroboration of 1,3-dienes

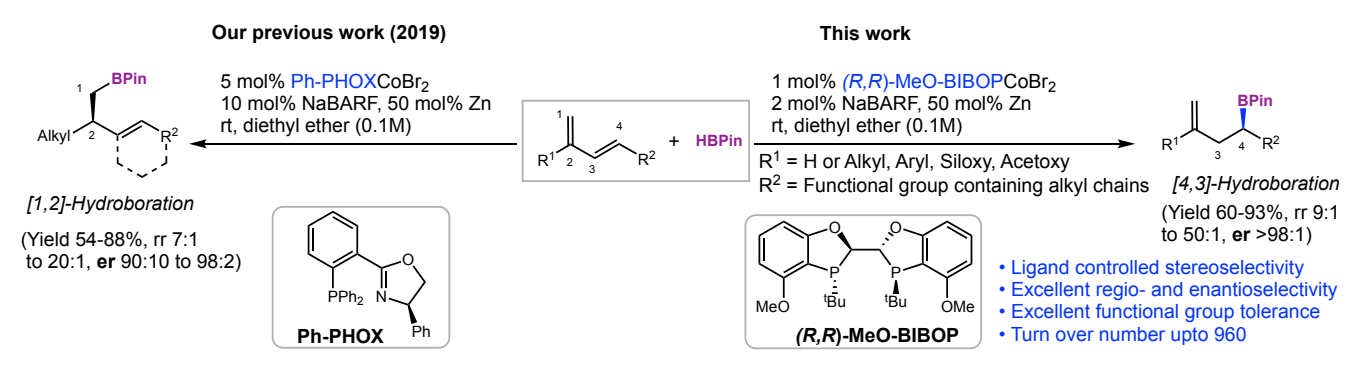


**Figure 1. A.** Importance of chiral secondary boronates prepared via HBPin or other borane sources. **B.** Regioselectivity conventions used in this paper (ref 5). **C.** Examples of uncommon hydroboration at C<sub>4</sub> of a 1,3-diene. **D.** Ligand control in Co-catalyzed [1,2]- vs [4,3]-hydroboration of 1,3-dienes (this work).

Since there is a dearth of reports on the synthesis of the versatile enantiopure secondary homoallylic boronates from readily available aliphatic 1,3-diene precursors, we wondered if ligand control could be exercised in the cobalt-catalyzed hydroboration to achieve such unusual [4,3]-addition of HBPin to 1,3-dienes (see Figure 1 B for numbering conventions used in this paper for specifying regioselectivity<sup>5</sup>). This paper documents our efforts in the area which culminated in the identification of several ligands including MeO-BIBOP (Figure 2), that gave high regio- and enantioselectivities for [4,3]-hydroboration products from 2,4-disubstituted as well as linear mono-substituted 1,3-dienes ( $R^1$  = alkyl or H, Figure 1 **D**). Accompanying computational studies provide key insights into the overall mechanism of these reactions and elucidate the possible origins of the observed regio- and enantioselectivities.

### RESULTS AND DISCUSSION

Experimental optimization of regio- and enantioselective 4,3-hydroboration of 2,4-disubstituted 1,3-dienes. We started the optimization studies with hydroboration of a prototypical 1,3-diene, (E)-2-methyl 1,3-octadiene (1a) using pinacolborane (HBPin) under conditions known to generate a cationic Co(I)-catalyst (LCoBr<sub>2</sub>/Zn/NaBARF). 10,14 This reaction gave varying amounts of products corresponding to [4,3]-(2a), [4,1]-(2b), [1,4]-(2c) and [1,2]-(2d) addition of the borane (Table 1). In a systematic examination of ligand effects, more than 40 ligands were explored, and the most significant results are shown in Table 1. A more complete list of ligands and their effect on selectivities are included in the Supporting Information (Table S1, p. S37). Systematic examination of solvents revealed that while methylene chloride and diethyl ether were acceptable, the latter was found to be the solvent of choice with minimal side reactions, especially for the formation of the [4,1]-adduct 2b with some of the ligands (vide infra). Among the activators NaBARF was found to be the best choice for the generation of a cationic Co(I) intermediate, which is presumed to be the active catalyst in these reactions (Table S2-S3, p. S39).<sup>10, 14</sup> Examination of the results in Table 1 reveals that unlike the phosphinooxazoline ligands which gave mostly the [1,2]-hydroboration product (2d) irrespective of the substitution pattern of the phosphine on the oxazoline ring, 10 chelating bis-phosphines have a dramatic effect on the regioselectivity of the hydroboration process depending on the backbone scaffolding. Most common achiral 1,n-bis-diarylphosphinoalkanes (dppm, dppe, dppp) and ligands like dpppbz, DPEPhos and XantPhos, gave the [1,2]-hydroboration product (2d) in greater that 90% selectivity over other regioisomers (Table 1, entry 1). See Supporting Information for the names and structures of the ligands (Figure S1, p. S38) and Table S1 (p. S37) for a more complete list of selectivities, as seen with other ligands. 1,1'-Diphenylphosphinoferrocene (dppf) showed the formation of the uncommon [4,3]-hydroboration product along with the 1,2-adduct (2a:2d = 40:58, en-Likewise, bis-1,2-dicyclohexylphosphinoethane (dcype) gave nearly 1:1 regioselectivity for the [4,3]- and [1,2]- hydroboration products (entry 3). Among the chiral catalysts, the Co-complex of (S,S)-BDPP gave a comparable proportion (up to 40%) of the 4,3-hydroboration product along with exceptionally high enantioselectivity (er >99:1; Table 1, entry 4). These results prompted us to initiate an exhaustive screening of various other chiral *bis*-phosphine ligands (Figure 2) with the goal of achieving high regio- and enantioselectivities for the [4,3]-adduct **2a**.

Table 1. Ligand Effects on Regio- and Enantioselective Hydroboration of 2-Methyl 1,3-octadiene (1a)<sup>a</sup>

$$\begin{array}{c} \text{HBPin (1.05 equiv)} \\ \text{5 mol\% Co(L)Br}_2 \\ \text{10 mol\% NaBARF} \\ \text{50 mol\% Zn} \\ \text{rt, diethyl ether (0.1M)} \end{array} \begin{array}{c} \text{Me} \\ \text{1} \\ \text{1} \\ \text{2} \\ \text{2} \\ \text{3} \end{array} \begin{array}{c} \text{1} \\ \text{4} \\ \text{BPin} \\ \text{4} \\ \text{C}_4 \text{H}_9 \end{array} \begin{array}{c} \text{H} \\ \text{BPin} \\ \text{C}_4 \text{H}_9 \end{array} \begin{array}{c} \text{H} \\ \text{BPin} \\ \text{C}_4 \text{H}_9 \end{array} \begin{array}{c} \text{H} \\ \text{BPin} \\ \text{C}_4 \text{H}_9 \end{array} \begin{array}{c} \text{H} \\ \text{C}_4 \text{H}_9 \end{array} \begin{array}{c}$$

entry	ligand (L)	time (h)	conv. (%) <sup>b</sup>	regioisomeric ratio <sup>b</sup> <b>2a</b> [4,3]: <b>2d</b> [1,2]: <b>2b+2c</b>	er of 2a <sup>c</sup>
1	dppp	0.5	100	4:94:2	rac
2	dppf	15	100	40:58:2	rac
3	dcype	6	100	44:49:7	rac
4	(S,S)-BDPP	0.5	100%	40:60:0	>99:1( <i>R</i> )
5	Josiphos-1	6	100%	47:30:11	nd
6	Josiphos-2	0.5	100%	72:24:4	>99:1
7	(R,R)-Me-BPE	1	100%	29:71:0	82:18
8	(R,R)-Et-BPE	1	100%	38:62:0	95:5
9	(S,S)-Et-DuPhos	12	100%	26:69:5	94:6
10	(R,R)-iPr-DuPhos	2	100%(74%)	82:4:14	>99:1(S)
11	(R)-QuinoxP*	1	100%	75:9:15	>99:1( <i>R</i> )
12	(S,S)-BenzP*	0.5	100%(70%)	77:8:15	>99:1( <i>S</i> )
13	(1R,2S)-Daunphos	0.5	100%(81%)	91:5:4	>99:1( <i>R</i> )
14	(R,R)-BABIBOP	9	100%	90:7:3	97:3
15	(R,R)- $t$ Bu-BIBOP	0.5	100%	53:20:27	>99:1
16	(R,R)-Ph-BIBOP	6	100%	1:2:96	nd
<b>17</b> <sup>d</sup>	(R,R)-MeO-BIBOP	0.5	100%(82%)	98:1:1	> <b>99:1</b> ( <i>S</i> )

a. See SI Procedure A (p. S29) for experimental details. See Figure 2 for structures of the ligands. See also Figure S1 in SI, p. S38. b. Conversion and regioisomeric ratios were determined via GC-FID. In parentheses are the isolated yields for major product, **2a**. c. Enantiomeric ratios were determined via CSP-GC (Cyclosil B column) where baseline separation of boronates was observed. d. 1 equivalent of HBPin and 1.1 equivalent of 1,3-diene were used with 1 mol% catalyst, 2 mol% NaBARF, 50 mol% Zn.

Among ferrocene-derived chiral ligands Josiphos-2 (entry 6) gave a good level (72%) of regioselectivity for the [4,3]hydroboration product with excellent enantioselectivity (er >99:1). Ligands in the bis-phospholano-series, 1,2-bis-phospholanoethanes,  $\lceil (R.R) - \text{Me-BPE}$  and  $\lceil (R.R) - \text{Et-BPE}$ , entries 7 and 8] gave only modest regioselectivity but good enantioselectivity. Structurally related 1,2-bis-phospholanobenzenes, [(S,S)-Et-DuPhos and (R,R)-iPr-DuPhos, entries 9,10] gave modest to good regioselectivity, with the (R,R)-iPr-DuPhos (entry 10), giving up to 82% of the [4,3]-hydroboration product along with excellent enantioselectivity (er >99:1). However, significant amounts of the isomerization product 2b was also formed in this case. Three other ligands (entries 11-13, see SI p. S126-S128 for CSP GCs showing enantiomer separations) which give er >99:1 for the [4,3]-adduct are QuinoxP\*, BenzP\* and Duanphos, with the last one also showing excellent regioselectivity (>91% of the [4,3]-isomer). Recognizing that ligands with small bite angles (as calculated from the solid-state structure of the LCoBr<sub>2</sub> complexes: QuinoxP\* 91.29°; BenzP\* 87.38°; Duanphos 87.68°; (R,R)-iPr-DuPhos 89.02° versus (S,S)-BDPP 97.30°)<sup>15</sup> tend to give better selectivity, we turned to a series of tunable benzooxaphosphole (BIBOP) ligands<sup>16</sup> with the hope of further improving the regioselectivity (entries 14-17). While the parent system with only a t-butyl P-substituent (t-Bu-BIBOP) gave only a modest regioselectivity (entry 15), a 4,4'-dimethoxy derivative (entry 17, bite angle 87.41°) was outstanding in delivering exceptionally high regio- (rr = 98:2) and enantioselectivity (er >99:1) for the 4,3-adduct [GC: SI, p. S115; CSP GC: SI, p. S126). Anecdotally, we also observed that the successful ligands, which yielded high selectivities (BenzP\*, Duanphos, t-Bu-BIBOP, MeO-BIBOP) also have outstanding catalytic activities. Finally, a BIBOP ligand with a biaryl motif, BABIBOP (entry 14) also gave acceptable levels of selectivity (rr 90:10 and er 97:3), but the reaction was found to be unusually slow (9 h under otherwise identical conditions versus  $\sim 0.5$  h with catalysts such as with ligands t-Bu-BIBOP, MeO-BIBOP). Indeed, the catalyst prepared from MeO-BIBOP also showed outstanding reactivity with as little as 1 mol% [MeO-BIBOP]CoBr2, 2 mol% NaBARF and 50 mol\% Zn for the reaction to complete in 30 minutes, along with excellent regio- and enantioselectivities. Given longer reaction times (48 h), this reaction can be carried out on a 2gram scale, with 0.1 mol% of the catalyst giving 96% isolated yield (vide infra Figure 4 A Eq 1).

Table 2. Cobalt Sources and Other Reducing Agents

HBPin (1.0 equiv.)
$$(R,R)-\text{MeO-BIBOPCoX}_2 \text{ (1mol\%)}, \\ \text{NaBARF (x mol\%)}, \\ \text{reductant (x mol\%)}, \\ \text{diethyl ether (0.1M), rt, time} \\ \textbf{1a (1.1 equiv.)} \\ \textbf{Me} \\ \text{NaBARF (x mol\%)}, \\ \text{Hopping the properties of the pr$$

no.	X in CoX <sub>2</sub>	reductant	NaBARF	time	conv.	regioselectivity	er of
		(mol%)	(mol%)	(h)		[4,3]:[4,1]:others	[4,3]
1	acac	none	0	24	40	1:2:97	
2	acac	Zn (50)	0	24	50	1:2:97	
3	acac	none	2	1	100	98:1:<1	>99:1
4	acac	Zn (50)	2	0.5	100	98:2:0	>99:1
5	OAc	Zn (50)	2	2	100	98:2:0	>99:1
6	Br	none	0	24	0		
7	Br	none	2	1.5	100	98:2:0	>99:1
8	Br	Zn(5)	2	0.5	100	98:2:0	>99:1
9	Br	Li <sub>3</sub> N (20)	2	0.5	100	98:2:0	>99:1
$10^{a}$	Br	TMS-Py(5)	2	0.5	100	97:3:0	>99:1

a. TMS-py: 1,4-bis(trimethylsilyl)1,4-dihydropyrazine

Co-Precursors and Reducing Agents. Since it is known that in some cobalt-mediated hydroboration reactions using Co(OAc)<sub>2</sub> or Co(acac)<sub>2</sub> complexes as precursors instead of the halides, HBPin itself can act as a reducing agent for the Co(II) complex,<sup>17</sup> we briefly examined these precursors, and the results are shown in Table 2 (entries 1-5). For details, see Table. S7, p. S41. Thus  $LCo(acac)_2$  complex (L = (R,R)-MeO-BIBOP) in the absence of Zn or NaBARF, catalyzed the HBPin addition to the typical substrate (E-2-methyl-1,3-octadiene) in a sluggish reaction (<50% conversion, 24 h, rt) giving a mixture of regioisomeric products in which the desired 4,3-adduct 2a was only a minor component (entries 1 and 2). Most interestingly, the LCo(acac)2 complex in the presence of 2 mol% NaBARF (no Zn!) gives 82% of the 4,3-adduct in an er of >99:1 in 1 h at room temperature (entry 3). In previous work, we have seen similar reactivity (i. e., reaction in the absence of Zn) in 1,2-hydroboration of 1,3-dienes with (L)Co(Cl)<sub>2</sub> [L = dppp, Ph-PHOX, Figure 1 **D**). Addition of 50 mol% Zn along with 2 mol% NaBARF accelerates the reaction giving comparable yield in much shorter time (entry 4) and these conditions were found to be the most optimal. Under identical conditions, the corresponding LCo(OAc)<sub>2</sub> complex behaved similarly, giving 80% yield of the product in 2 h (entry 5).

Effect of different reducing agents for the reduction of the  $LCoBr_2$  complex is shown in entries 6-10. See Table S6, p. S41. In the absence of any reducing agent and NaBARF there is no reaction (entry 6). As expected, NaBARF alone (2 mol%) in the presence of HBPin is a viable option giving a relatively slow reaction (entry 7). Presumably the cationic Co(II) complex formed under these conditions could be reduced by HBPin. Two other reagents we found useful for this reduction are  $Li_3N^{18}$  and 1,4-bis(trimethylsilyl)1,4-dihydropyrazine (Mashima's reagent)<sup>19</sup> as shown in entries 9 and 10. In the end we chose Zn based on its cost, availability, and ease of use.

### Partial list of Ligands investigated in hydroboration of 1,3-dienes

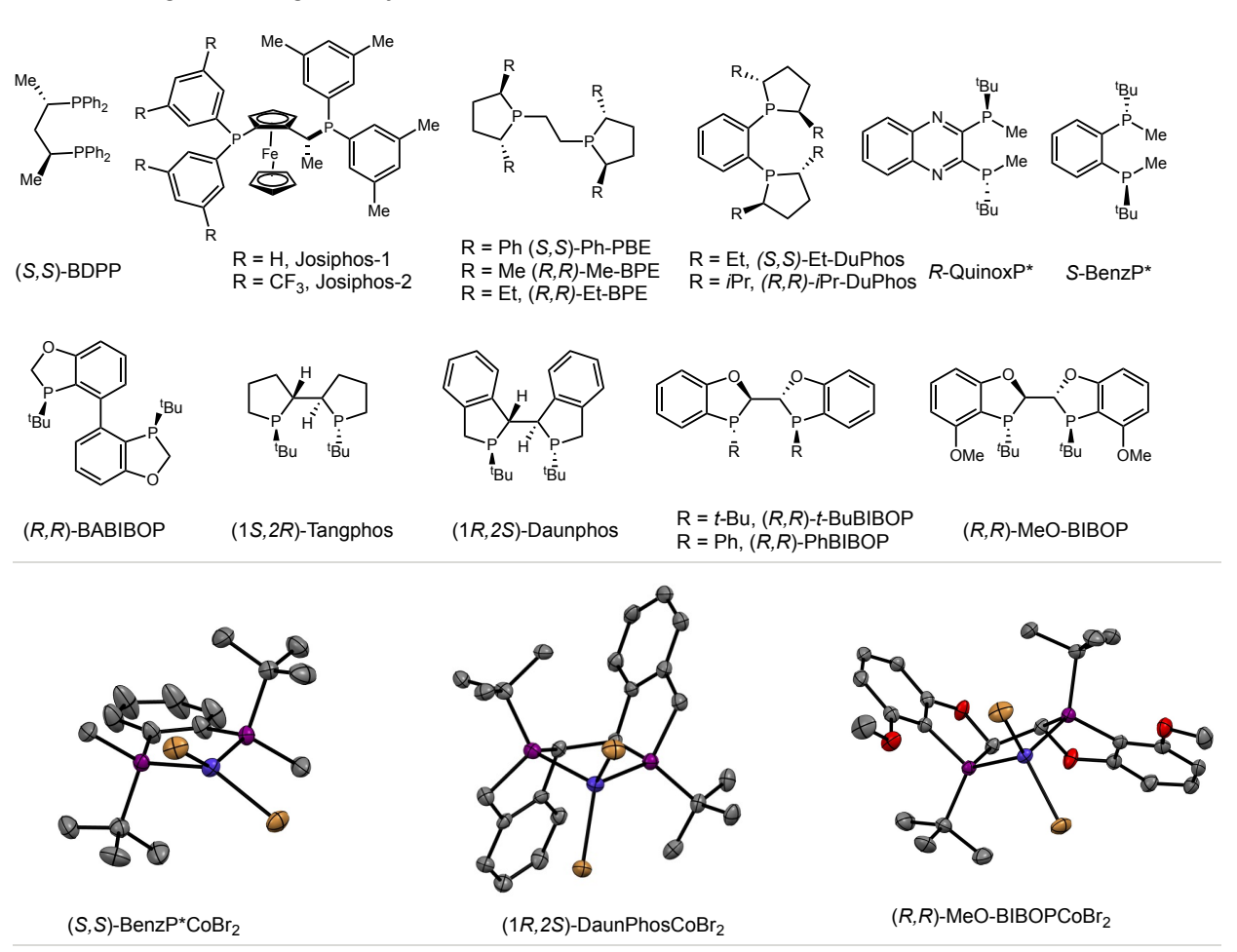


**Figure 2.** Partial list of chiral bis-phosphine ligands investigated for enantioselective hydroboration of 1,3-dienes. For a full list see SI, Figure S1, p. S38. Solid-state structures of the best precatalysts  $LCoBr_2$  [L = (S,S)-BenzP\*, (1R,2S)-Daunphos, (R,R)-MeO-BIBOP]. These structures have been deposited at CCDC and have the following numbers: 2151426, 2151424, 2151425 in order. While this article was under review, structure 2151426 ( $LCoBr_2$  [L = (S,S)-BenzP\*] was recently disclosed by us (see ref. 15).

Scope of substrates in the enantioselective [4,3]-hydroboration of 2,4-disubstituted 1,3-dienes. After we identified (R,R)-MeO-BIBOP as the most suitable chiral ligand for the highest overall selectivities in the [4,3]-hydroboration of a 2,4-disubstitued 1,3-diene, we set out to explore the scope of this reaction under the optimized condition. The results are shown in Figure 3. Various primary, secondary alkyl and cycloalkyl substituents at the 2-position of 1,3-octadiene and 1,3-nonadiene were explored for hydroboration with HBPin. Good yields of the 4,3-hydroboration products (2-4) were obtained nearly as a pure regioisomer (rr >95:5) with excellent enantioselectivity (er >99:1). The enantiomeric ratios of the products were determined by CSP GC of the boronate itself, the alcohol derived via perborate oxidation of the boronate, or the corresponding acetate from the alcohol (Scheme 1, see Supporting Information for details, Procedures G and H, p. S34-S35).

Products from 2-silyloxy (**5**) and 2-acetoxy (**6**) dienes show that these sensitive functional group can survive under our reaction conditions, which are relatively more tolerant as compared to the corresponding copper-catalyzed protoboration,  $^{9,13}$  which are carried out with up to 40 mol% of t-BuOK. Both the silyl enol ether (**5**) and the enol acetate (**6**) are formed in excellent regio-and enantioselectivity.

# Scheme 1. Derivatization of the boronate for determination of er

$$\begin{array}{c} \text{R}^{1} \\ \text{R}^{1} \\ \text{R}^{2} \\ \end{array} \begin{array}{c} \text{NaBO}_{3} \text{ (3 equiv.),} \\ \text{THF:H}_{2}\text{O} \text{ (1:1, 0.1M)} \\ \text{2 h to 24 h, rt} \\ \end{array} \begin{array}{c} \text{R}^{1} \\ \text{R}^{1} \\ \text{OAc} \\ \end{array} \begin{array}{c} \text{Ac}_{2}\text{O, DMAP,} \\ \text{Et}_{3}\text{N, CH}_{2}\text{Cl}_{2} \\ \text{3 h to 24 h, rt} \\ \end{array} \begin{array}{c} \text{R}^{1} \\ \text{COAc} \\ \text{R}^{2} \\ \end{array}$$

The enantioselectivity in the enol acetate 6 was measured on an acetyl migration product, (S)- 4-acetoxy-oct-2-one (SI, p. S54, S147-S150), formed upon oxidative cleavage of the boronate 6. The products (7-i-7-iii) show that aryl and heteroaryl (thiophene and indole) groups are acceptable at the 2position. For further elaboration of the primary hydroboration products into other derivatives including cyclic motifs, substituents on the 4-alkyl chain are important and products with such substitution are illustrated with examples 8-14 in Figure These substrates also show the remarkable functional group compatibility of the hydroboration conditions. Thus a 4-methoxyphenyl-thioether (8) and a 2-bromophenyl ether (9) are tolerated and the products are formed with excellent regioand enantioselectivity in each case. Remarkably a chloroalkyl substituent on C<sub>4</sub> has no adverse effect on the efficiency or selectivity of the 4,3-hydroboration (10). An unprotected hydroxyl group on the sidechain is acceptable even though the yield of the reaction is somewhat reduced under the standard conditions. The corresponding -OTBS ether or the mesylate restores the reactivity and very good yields of the corresponding [4,3]-adducts are obtained (12, 13). Only a single enantiomer is seen in most of these reactions. Surprisingly an azide functionality is tolerated in this reaction (14).

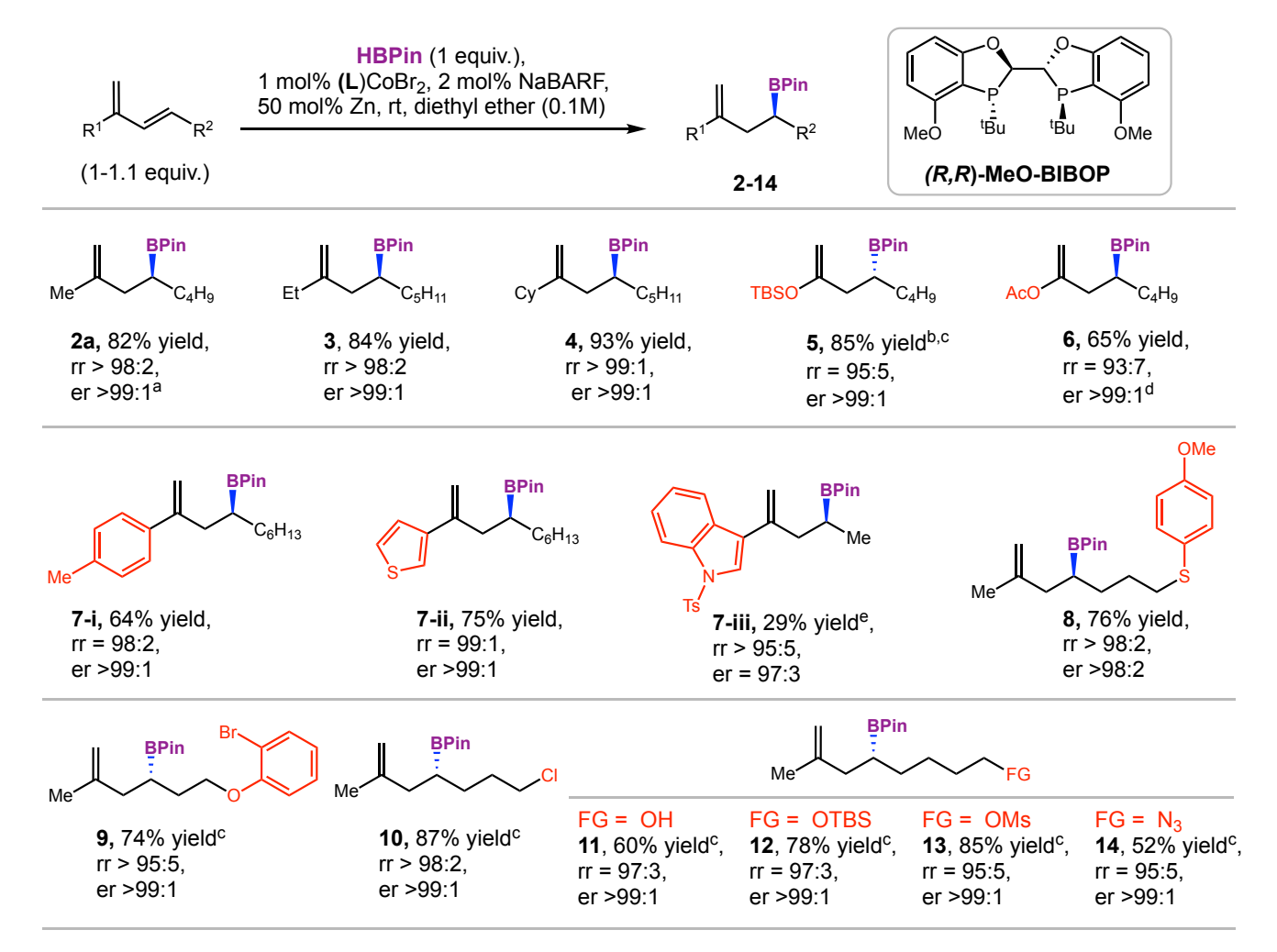


**Figure 3.** Scope of substrates in hydroboration of 2,4-disubstitued 1,3-dienes. See Supporting Information for experimental details. er determined by CSP GC of the boronate, the alcohol derived from the boronate or the corresponding acetate (Scheme 1). a. Absolute configuration of **2a** was determined by conversion into the corresponding alcohol whose specific rotation was compared to that of an authentic sample (see SI, p. S48)<sup>20</sup> Those of other boronates were assigned by analogy. See Supporting Information for details. b. Yield was determined by NMR. c. (S,S)-MeO-BIBOP was used. d. er determined on (S)-4-acetoxy-octan-2-one which is formed upon oxidation of the boronate **6** (see SI, p. S54). e. 3 mol% of (R,R)-MeO-BIBOP was used.

Gram-scale synthesis. The [(MeO-BIBOP)Co]<sup>+</sup> [BARF]<sup>-</sup>catalyzed [4,3]-hydroboration is a very efficient reaction that can be carried out on a gram scale using as little as 0.1 mol% of the catalyst. Under the conditions shown in Figure 4 A, the [4,3]-hydroboration product from (E)- 2-methyl-1,3-octadiene is formed almost exclusively as a single regioisomer (96%), isolated by simple filtration of the crude product over silica gel (see SI, p. S33).

The [4,1]-hydroboration product. Solvent effect, diethyl ether vs CH<sub>2</sub>Cl<sub>2</sub>. A remarkable solvent effect was observed in the [(MeO)BIBOP]Co]<sup>+</sup>-catalyzed reaction. When the reaction was carried out in diethyl ether and with low concentrations of the catalyst, 97% of the [4,3]-hydroboration product 2a was obtained. Under similar conditions, but with higher concentration of the catalyst, and in CH<sub>2</sub>Cl<sub>2</sub> up to 95% of the [4,1]-product 2b was observed (Figure 4 B, see SI, p. S70, p. S188-S192). The enantioselectivities for both products 2a and 2b remain at er >99:1 (see SI, p. S190). Indeed, isolated 2a can

be readily isomerized into **2b** under the reaction conditions in CH<sub>2</sub>Cl<sub>2</sub>. (Figure 4 **C**). The structure and absolute configuration of the alcohol (*S*)-(–)-derived from [4,1]-product **2b** was confirmed by comparison of spectral characteristics and specific rotation with those of an authentic sample described in the literature.<sup>21</sup>

An Application. Synthesis of a C<sub>1</sub>-methallyl pyranoside. Past applications of several allyl and homoallyl alcohol intermediates prepared during this study for the synthesis of polyketides and other molecules are mentioned in the text in connection with the establishment of absolute configuration of these products. A straight-forward synthesis of an enantiomerically pure methallyl pyranoside (Figure 4 **D**, 15) further illustrate one of the myriad of possibilities for the use of functionalized boronates for the synthesis of cyclic derivatives.

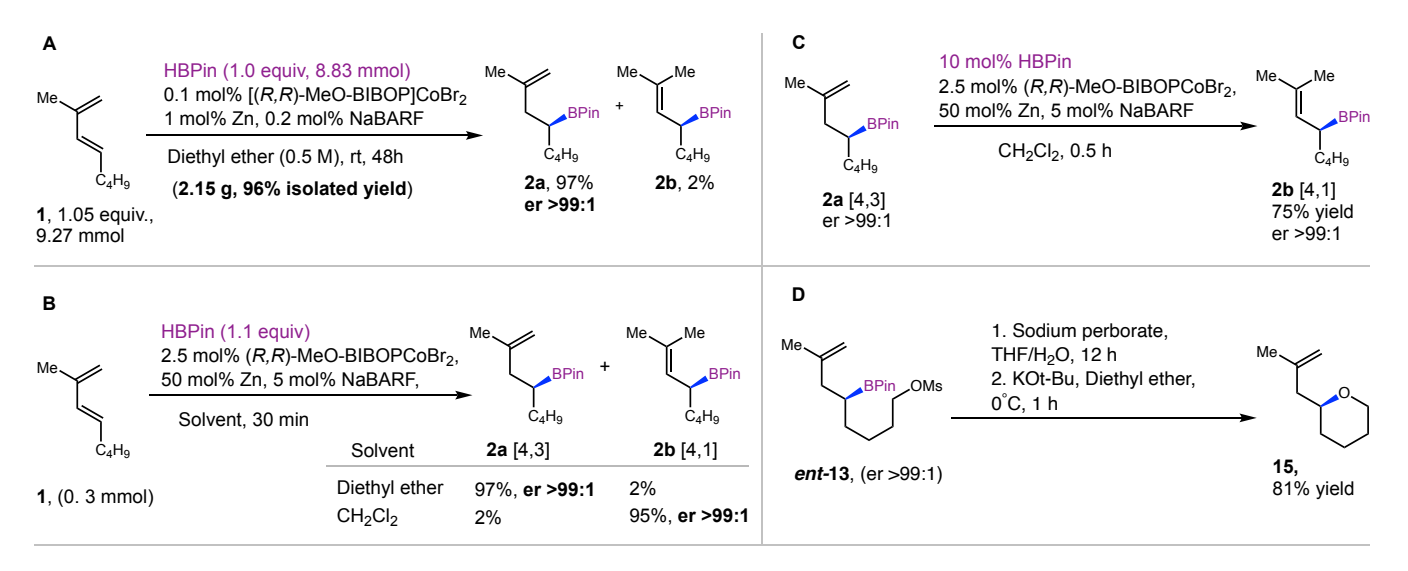


**Figure 4. A.** Gram-scale hydroboration of 1,3-dienes. **B.** Solvent effect on regionselctivity. Synthesis of [4,1]-hydroboration product in  $CH_2Cl_2$ . **C.** Isomerization of [4,3]- adduct into [4,1]-adduct. **D.** Use of functionalized boronates for the synthesis of a cyclic derivative.

Enantioselective [4,3]-Hydroboration of Terminally Substituted 1,3-Dienes. Terminal mono-substituted 1,3-dienes with a substituent at the C<sub>4</sub> position (by the convention defined in this paper)<sup>5</sup> are among the most readily available precursors.<sup>22</sup> Enantioselective hydroboration in this class of prochiral compounds using HBPin, with boron incorporation on an internal carbon ('Markovnikov' addition) is not known; however a related Pt-catalyzed enantioselective [4,1]-diboration using B<sub>2</sub>(Pin)<sub>2</sub> has been reported by Morken.<sup>23</sup> As for the hydroboration with base metal catalysts, previous work including our own had shown that with common bis-phosphine and phosphino-oxazoline ligands mostly achiral [1,2]- and [1,4]-hydroboration products were formed in this reaction. 8a,8c,8d,8g,10,24 We wondered if the cobalt-complexes of the new ligands introduced in the present work for the [4,3]-hydroboration of 2,4-disubstituted 1,3-dienes would also give the unusual [4,3]-regioselectivity in the linear dienes thus providing access to nearly enantiopure secondary boronates that can be converted into homoallyl alcohols and other useful synthons which are widely used intermediates in synthesis. Delightfully, we find that indeed this is the case, and ligands with narrow bite angles, yield significant amounts of the 4,3hydroboration product 17a from (E)-nona-1,3-diene (16), as shown in Table 3. Thus QuinoxP\*, BenzP\*, Duanphos and i-PrDuphos gave nearly 1:1 mixture of the uncommon 4,3-adduct 17a along with an achiral [1,2]-adduct 17d. The structure of the secondary, homoallylic boronate (17a), was confirmed by comparison of its spectral characteristics with those of a product prepared by an alternate route (from vinyl boronate and allyl phosphate, 5 mol\% Cu catalyst vis-\(\delta\)-vis from (E) nonadiene and HBPin with 0.1 mol% Co in the present route) described in the literature.<sup>25</sup> Finally, as with 2,4-disubstitued 1,3-dienes described earlier (Table 1, entry 17), (R,R)-MeO-BIBOP gave up to 75% of the [4,3]-hydroboration product with an er >99:1, along with 24% of the other regio-isomers (entry 8).

Table 3. Ligand effects on regio- and enantioselective hydroboration of (E)-1,3-nonadiene<sup>a</sup>

$$\begin{array}{c} & \text{HBPin (1.05 equiv)} \\ & 5 \text{ mol% Co(L)X}_2 \\ & 10 \text{ mol% NaBARF} \\ & 50 \text{ mol% Zn} \\ & \hline \text{rt, diethyl ether (0.1M)} \end{array} \\ & \textbf{H} \\ & \begin{array}{c} \text{BPin} \\ \text{C}_5\text{H}_{11} \end{array} \\ & \begin{array}{c} \text{H} \\ \text{BPin} \end{array} \\ & \begin{array}{c} \text{H} \\ \text{H} \\ \text{C}_5\text{H}_{11} \end{array} \\ & \begin{array}{c} \text{C}_5\text{H}_{11} \\ \text{C}_5\text{H}_{11} \end{array} \\ & \begin{array}{c} \text{T7c [1,4]} \end{array} \\ & \begin{array}{c} \text{17d [1,2]} \end{array} \end{array}$$

entry	Ligand L	time (h)b	regioisom. Ratio	er of 17a
			17a [4,3]:17d [1,2]:others	
1	dppp	0.5	5:78:15	rac
2	dcype	0.5	8:45:45	rac
3	(S,S)-BDPP	0.5	16:75:9	90:10
4	(R)-QuinoxP*	0.5	40:54:6	>99:1
5	(S,S)-BenzP*	0.5	45:45:10	>99:1
6°	(1R 2S)-Daunphos	0.25	46:45:7	98:2
7	(R,R)-i-PrDuPhos	1	42:51:17	>99:1
8°	(R,R)-MeO-BIBOP	0.25	75:3:21	>99:1

a. See Supporting Information for details. b. Time for 100% conversion. c. For entries 6 and 8: 1 mol% (L)CoBr<sub>2</sub>/2 mol% NaBARF/ 50 mol% Zn.

Since [4,3] ('Markovnikov')-regioselectivity in hydroboration of linear dienes has not been reported before, other monosubstituted linear 1,3-dienes were explored under the optimized reaction conditions (1.0 mol\% [(R,R)-MeO-BIBOP]CoBr<sub>2</sub>, 2-5 mol% NaBARF and 50 mol% Zn, rt, in diethyl ether) and the results are shown in Figure 5. It was found that primary alkyl chains, as the R<sup>1</sup> substituent (Figure 5), such as pentyl (17) and methyl (18), at the 4-position of the 1,3-diene lead to good levels of [4,3]-hydroboration with minor amounts of other regioisomers. As before, enantioselectivities for the [4,3]-products were excellent (er >99:1). The product 17 has been used as an intermediate for the synthesis of S-Massoialactone. 25a Excellent chemoselectivity was observed for the hydroboration of a 1,3-diene (19) which was tethered to a free terminal alkene, demonstrating the ability of the [L][Co(I)]<sup>+</sup> catalyst to selectively hydroborate the 1,3diene over a free alkene, along with good regioselectivity (81:19) and excellent enantioselectivity (er >97:3). Alkyl chains carrying silyl ethers, such as 20 (OTBS) and 21 (OTBDPS) which are ubiquitous in polyketide synthesis, are tolerated well on the 1,3-diene, with good regioselectivities and excellent enantioselectivities (er >97:3). The structures and configurations of the homoallyl alcohols from secondary boronates 20 and 21 were confirmed by comparison of spectral properties and specific rotations of authentic intermediates as reported by Sestilo<sup>26</sup> and Smith<sup>27</sup> in their synthesis of (-)-Barrenazin A and (+)-Zampanolide respectively. Benzyl substitution at the C<sub>4</sub> position is tolerated as exemplified by the straight forward synthesis of known boronate adducts 22<sup>2b</sup> and 23.25a A different boronate structurally related 22 has been used as an intermediate for the synthesis of a lignan natural product, enterolactone. 2b Even though the regioselectivities in linear 1,3-dienes do not reach the levels seen in 2,4disubstituted dienes (Figure 3), the alcohol product from the oxidative cleavage of the boronate can be readily purified by column chromatography, thus providing a facile route to these highly versatile homoallylic alcohols. Finally, the example **24** illustrate the use of this chemistry for a double hydroboration of a linear 1,3-diene, which proceed in very good yield and excellent enantioselectivity. The enantiomeric ratio (er 98:2) of the product was ascertained by CSP GC after conversion of the diboronate to a diol and subsequently to a diacetate.<sup>28</sup> This route provides an attractive alternate to the related Morken's Pt-catalyzed enantioselective diboration of linear 1,3-dienes.

Finally, a class of substrates that was found to give none of the '4,3'-hydoboration products was 4-aryl substituted terminal 1,3-dienes like (E)-phenyl-1,3-butadiene. The major product (85%, rr >99:1) for this substrate resulted from a 1,2-hydroboration, using the (S,S)-BenzP\* complex. This compound and a close analog, (E)-2-methyl-4-phenyl-1,3-butadiene, surprisingly, failed to react under reaction with (R,R)-(MeO)BIBOP-complex (Figure 5, highlighted).

A preparative scale reaction of (E)-1,3-nonadiene under conditions, as described in Scheme 2 gave (S)-(-)-non-1-en-4-ol [(25) [ $\alpha$ ] $_D^{25.4} = -8.4$  (c 1.0 in CHCl $_3$ ; 97% ee)] in 59% isolated yield after oxidation and column chromatographic purification. The enantiomer (R)-(+)-non-1-en-4-ol [[ $\alpha$ ] $_D^{24} = +9.00$  (c 1.0 in CHCl $_3$ ; 96% ee)] prepared by a stoichiometric Brown allylation, has been described in the literature.

Scheme 2. Preparative scale synthesis of 25

### Enantioselective [4,3]-Hydroboration of Linear 1,3-Dienes<sup>a</sup>

**Figure 5.** Scope of substrates in [4,3]-hydroboration of linear dienes. a. See supporting information for details. er determined by CSP GC of the boronate, alcohol derived from the boronate or the corresponding acetate (Scheme 1). b. Using (*S,S*)-MeO-BIBOP.

Catalytic methods for  $\alpha$ -chiral homoallyl boronates. A close examination and comparison of this method with two other recently developed catalytic methods using pre-formed vinyl boronates, <sup>2b, 25a</sup> for the synthesis of  $\alpha$ -chiral homoallyl boronates reveal that our method is at least as competitive, yet uses, arguably, more user friendly precursors (dienes and HBPin versus vinyl boronates and other reagents like ArZnX or allylic phosphates). Other favorable factors might be higher turnover numbers in the catalysts, and, comparable, if not better enantioselectivities in most instances where such data is available.

Computational investigation of the mechanism: origin of regio- and enantioselectivities.

In order to rationalize the regio- and enantioselectivities observed in the hydroboration of 1,3-dienes, we chose two prototypical ligands (*R*,*R*)-BenzP\* and (*R*,*R*)-MeO-BIBOP, which, despite their widely different structures, gave very high regioselectivities and excellent enantioselectivities for the [4,3]-product in the hydroboration of a number of 2,4-disubstituted 1,3-dienes (Figure 6). Additionally, these ligands gave opposite enantiomers of the product, thereby providing an opportunity to validate the methods used in these calculations in two disparate ligand systems.

Extensive details of the computations are included in the Computational Supporting Information (CSI) and are referred to here under specific page numbers indicated as CSI p.SX.

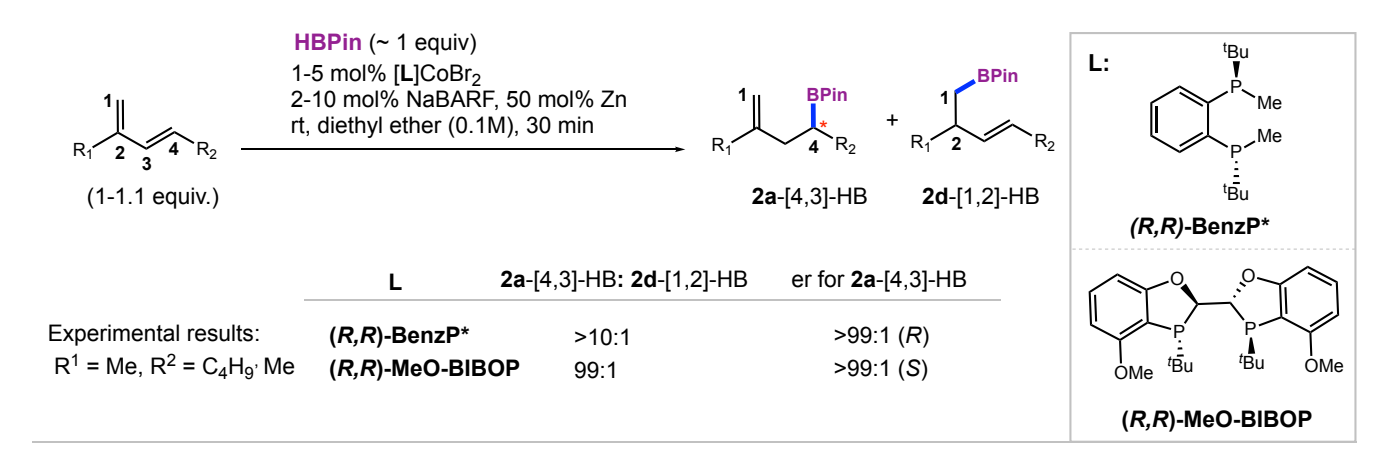


Figure 6. Ligand effects on regio- and enantioselectivity in 4,3-hydroboration of 1,3-dienes.

Computational methods. To gain further insight into the origin of the uncommon regio-and enantioselectivities in the hydroboration of 2,4-disubstituted 1,3-dienes, we utilized in silico methods, analyzing the overall mechanism of the reaction, as well as the individual intermediates and transition states in what emerged as a preferred pathway for the hydroboration from our initial investigations. Computations were performed using the Gaussian 16 suite of programs.<sup>29</sup> The geometries were optimized using the B3LYP-D3 hybrid density functional along with Pople's 6-31+G\*\* basis set for all atoms except for the transition metal (cobalt).30 For all basis sets, 5d functions were used. The Stuttgart-Dresden double-ζ basis set (SDD) with an effective core potential was used for cobalt.<sup>31</sup> All of the stationary points were characterized as minima or a first-order saddle point (transition state) by evaluating the corresponding Hessian indices. The transition states (TSs) were verified by examining whether the stationary point has a unique imaginary frequency representing the desired reaction coordinate. Moreover, Intrinsic Reaction Coordinate (IRC) calculations were carried out to further characterize the true nature of each TS structures.<sup>32</sup> The geometries obtained as the endpoints on the either side of the IRC trajectories were subjected to further optimization to identify the pre-reacting complexes and product intermediates. The zero-point vibrational energy (ZPVE), thermal, and entropic corrections obtained at 298.15 K with B3LYP-D3/6-31+G\*\*, SDD(Co) level of theory are included in the Gibbs free energies.<sup>33</sup> Furthermore, single-point energy calculations to explore solvation effects (SMD, Cramer-Truhlar continuum solvation model),<sup>34</sup> different functionals (e.g., B3LYP-D3, M06L, M06-D3, ωB97x-D and TPSSh) and basis sets (e.g., Pople's 6-311+G\*\* TZ basis set and Ahlrichs' def2-TZVP basis set) confirmed the predicted trends of regio- and enantioselectivities (see CSI Table S4, p. S18 and Figure S13, p. S30 for (R,R)-BenzP\* and Table S7, p. S33-34 and Figure S17, p. S44-45 for (R,R)-OMe-BIBOP).35 All geometries were optimized as closed-shell singlet states and the triplet energy profile was not considered.<sup>36</sup> It is worth noting that due to the sheer size of the BARFcounter anion, no coordination was anticipated and thus was not included in this computational study. For convenience of the computational calculations, we used (E)-2-methylpenta-1,3-diene as our substrate. Experimentally this substrate and (E)-2-methylocta-1,3-diene gave very similar results (Figure 6).

Computational investigation of plausible mechanisms. Four distinct possibilities of how this reaction might proceed are summarized in Figure 7 A through Figure 7 D, with more intimate details of the most viable (vide infra) Oxidative Boryl Migration route shown in Figure 8 (see also CSI Figure S2, p. S3). The starting cobalt complex, [P~P]CoBr<sub>2</sub>, when reduced by Zn in the presence of NaBARF, makes a 12-electron cationic Co(I) complex, which is presumed to be the active catalyst in this reaction. The diene is a good candidate for binding with cobalt as it makes a stable 16-electron complex (Figure 7 A).<sup>37</sup> Once this complex is formed, there is the possibility of an oxidative cyclization of the diene with the cobalt bound catalyst [(P~P)Co]+, thereby producing a five membered cobaltacycle intermediate (Figure 7 A). The formation of this complex could be followed by HBPin addition to form the products. Another possibility is that oxidative addition of HBPin to the cobalt(I)-complex,  $[Co(P \sim P)]^+$  occurs first to form a Co(III)-intermediate, which is followed by ligation of the 1,3-diene (Figure 7 B). Successive migratory insertions of the double bonds into either Co-hydrogen or Co-boryl group could lead eventually to the products seen in these reactions (Figure 7 B). While investigating these two mechanisms, we found that neither the Co(III)-metallacycle (Figure 7 A) nor the Co(III)(BPin)(H)-adduct (Figure 7 B) is likely to be an intermediate in these reactions. In an attempt to find a transition state for oxidative cyclization (Figure 7 A, see also CSI Figure S3a, p. S4), we found that the metallacycle reverted back to the stable initial structure, i.e., the diene bound in a  $\eta^4$  fashion, thus presenting no viable transition state for this reaction (CSI Figure S3b, p. S5). Neither could we locate any transition state for oxidative addition of HBPin with the catalyst (CSI, Figure S4a, p. S6). Repeating the same calculations with explicit solvation (SMD in solvent either DCM or diethyl ether) and a larger TZ basis set for oxidative addition of H-BPin and oxidative cyclization resulted in no change from what was calculated for the gas phase (Figure S3a, p. S4 and Figure S4b, p. S7). Indeed, we observed a different minimum with the oxygen atom of H-BPin coordinated to [(R,R)-BenzP\*|Co|+ that does not undergo further elongation of H-B bond for the cobalt atom to be inserted into this bond (see Figure S4b, p. S7). So, we excluded these routes (Figure 7 A) and Figure 7 **B**) from among the possible mechanisms.

### A: Oxidative cyclization of 1,3-diene to form cobalta-cycle intermediate

### B: Oxidative addition of HBPin to form [B-Co(III)-H]<sup>+</sup> intermediate

### C: Oxidative boryl-migration followed by reductive elimination to form C-H bonds

### D: Oxidative H-migration followed by reductive elimination to form C-B bonds

Figure 7. Plausible mechanisms of  $(L^*)[Co]^+$ -catalyzed hydroboration of 1,3-dienes showing all observed products.

We focused on the latter two possibilities (Figure 7 C and 7 D), originally proposed for a cationic Ru(II)-catalyzed transhydroboration of an internal alkyne.<sup>38</sup> This mechanism was recently invoked successfully by Chen et al.,<sup>39</sup> while discussing the origins of selectivities in the ligand dependent-HBPin addition to 1,3-dienes to give either [1,2]- or [1,4]-adducts as we reported in 2019.<sup>10</sup> In this reaction, ligands 2-(oxazolinyl)-phenyldiphenylphosphine (PHOX) or 1,2-bis-(diphenylphosphino)ethane (DPPE) gives [1,4]-adducts and, 1,3-bis-(diphenylphosphino)propane (DPPP) gives a [1,2]-adduct. In Figure 7 C and Figure 7 D, broad details of these mechanisms are shown in the context of the specific products ([4,3]-, [4,1]-, [1,4]-, and [1,2]- additions) that are formed in the hydroboration of 1,3-dienes (see also CSI Figures S9-S10,

p. S12-S14). We have considered all regio-isomeric products that are formed (Table 1) and the details are included in the **CSI**. In Figure 7C, the *Oxidative Boryl Migration* (**OBM**) from the newly formed  $[(P\sim P)\text{Co}(\text{diene})(\text{HBPin})]^+$  complex, followed by a reductive elimination with formation of the C-H bond is shown. Further details of this mechanism which involves an **OBM** that leads to the observed products, via [4,3]-and [1,2]-hydroborations, are shown in Figure 8. Thus, the cationic Co<sup>I</sup>-species **26**, leads to an  $\eta^4$ -diene complex **27** and, subsequently to a HBPin adduct **28**. The species **28** can undergo an **OBM** pathway that involves two steps, (i) boryl migration forming the C-B bond at either C<sub>1</sub> (leading to **29a**) or C<sub>4</sub> (leading to **29b**) of the diene. The C<sub>4</sub> addition generates a stereogenic center (at C<sub>4</sub>) and an  $\eta^3$ -allyl-cobalt hydride

species.<sup>40</sup> (ii) A reductive hydrogen migration from cobalt-hydride **29a** to the terminal carbons of  $\eta^3$ -allyl species,  $C_2$  or  $C_4$  will give either the 1,2-product **31a** (through **30a**) or 1,4-product (not shown since this product is not seen). Instead, if the **OBM** results in the migration of B to the  $C_4$  carbon, **29b** 

will result, which by subsequent reductive elimination can give the major observed product, [4,3]-hydroboration (31b through 30b) or a [4,1]-hydroboration by H-migration to  $C_1$  to give 31c (through 30c).

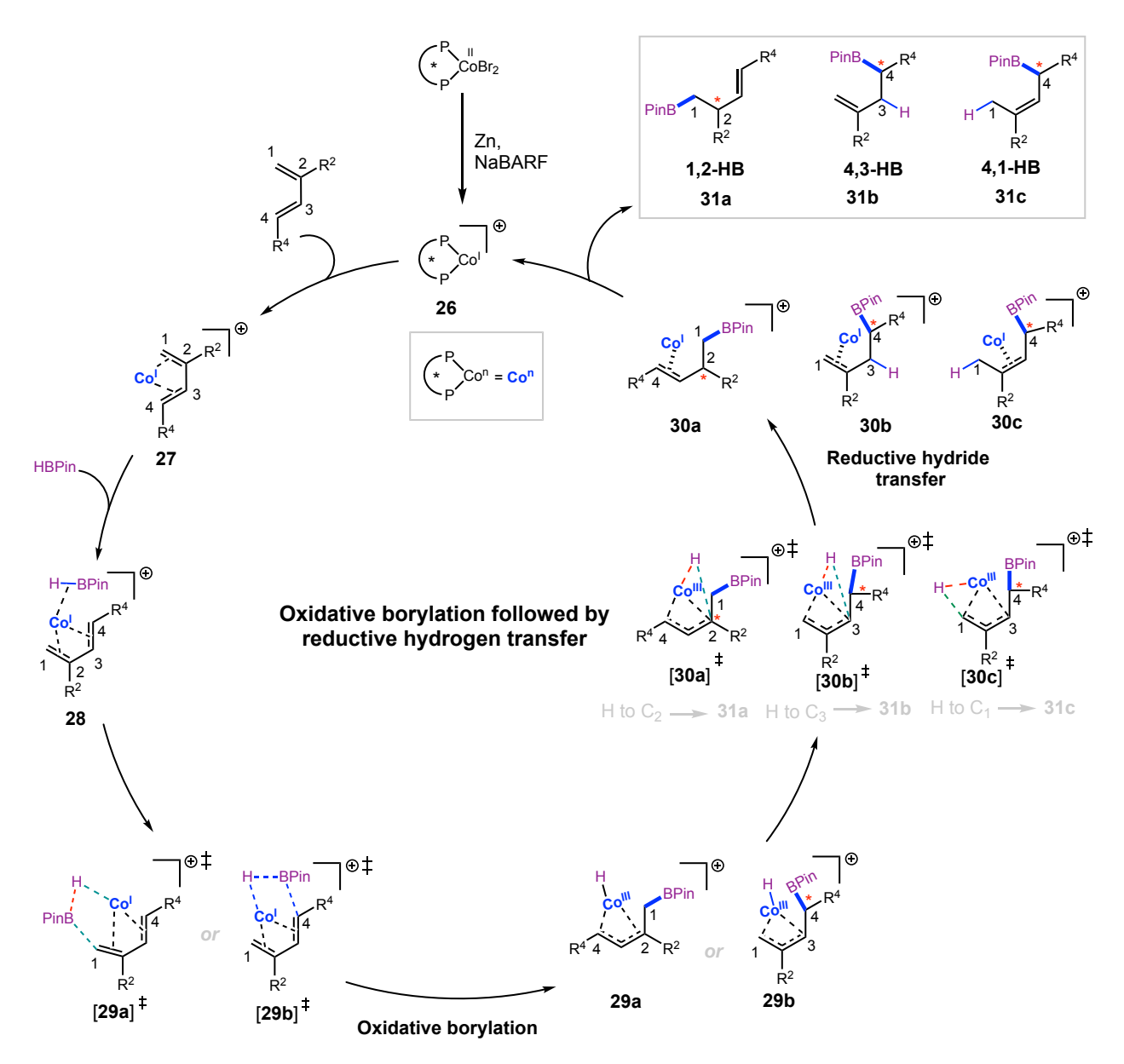


Figure 8. Details of Oxidative Boryl Migration (OBM) followed by C-H Formation by reductive elimination (also, see Figure 7 C).

An alternative is an initial *Oxidative Hydrogen Migration* (**OHM**) followed by reductive elimination to form the C–B bond (Figure 7 **D**). The details of this less likely process (vide infra) which result in [4,1]- and [1,4]-hydroboration products are shown in the **CSI** Figure S9, p. S12-S13. Figure S9 (p. S13) shows a side-by-side comparison of the **OBM** and **OHM** routes. The following numbers refer to structures in **CSI** Figure S9, p. S13. The **OHM** pathway follows a route starting with (i) oxidative hydrogen migration to the catalyst bound diene (Figure S9, **S1-3**) either to  $C_1$  (to give Figure S9, **S1-7a**) or to the  $C_4$  (to give Figure S9, **S1-7b**) position, thereby

breaking the B–H bond and forming a cobalt-boryl  $\eta^3$ -allyl species; and (ii) reductive boryl migration to either  $C_1$  or  $C_4$  will give Figure S9 **S1-8a** or **S1-8b**, which leads to the [4,1]-or [1,4]-hydroboration products, **S1-9a** and **S1-9b**, respectively.

**Prochiral Face Recognition.** Upon formation of the  $\eta^4$ -complexes with the cationic  $[(P \sim P)Co]^+$  catalyst, the prochiral dienes form diastereomeric complexes whose relative amounts could dictate selectivities in the subsequent reactions with HBPin. Since the cobalt complexes of (R,R)-BenzP\* and (R,R)-MeO-BIBOP ligands gave excellent regio- and

enantioselectivities in the hydroboration reactions, we started our studies with an examination of the possible diastereoselective binding of these catalysts to the prochiral faces of the diene using DFT methods [B3LYP-D3/6-31+G\*\*, SDD(Co)]. The results of these calculations are shown in the **CSI** Figure S5 and **CSI** Figure S6 and Table S2 (p.S8-S9). Thus with (*R*,*R*)-BenzP\*, the *re* face coordination of the diene (with respect to the prochiral C4 atom) was 1.8 kcal/mol lower in energy as compared to the *si* face coordination (Figure 9 **A**, see also **CSI** Figure S5 and Table S2, p.S8-S9). For (*R*,*R*)-MeO-BIBOP, on the other hand, a *si* face bound structure was energetically more favorable (Figure 10 A, see also Figure S6, **CSI** p.S9): this structure was 5.2 kcal/mol lower than the corresponding *re* face-bound complex (see **CSI** Figure S6 and Table S2, p.S8-S9).

Included in CSI Table S2 (p. S8) are the relative values of the two diastereomers **I**(re) and **I**(si) calculated using various levels of theory and basis sets including solvation (A - E). A= B3LYP-D3/6-31+G\*\* (gas phase, SDD for cobalt) level of SMD(DCM)/B3LYP-D3/6-311+G\*\*, theory. B: SMD(diethyl ether)/B3LYP-D3/6-311+G\*\*, D: SMD(DCM)/B3LYP-D3/def2-TZVP, E: SMD(diethyl ether)/B3LYP-D3/def2-TZVP. B. C. D. E are single-point energy calculations with those specific methods. There is a remarkable and consistent agreement between the various methods, thus validating the preference for the indicated diastereomers in each case.

In the next step after the initial diastereoselective recognition of re-face of the 2,4-disubstituted diene by the [(R,R)-BenzP\*Co]<sup>+</sup> (Figure 9 **A**), HBPin approaches the coordination sphere of the intermediate complexes [(R,R)-BenzP\*Co(diene)]<sup>+</sup> from where it is spatially most accessible (Figure 9**A**, see also **CSI** Figure S7 and Table S3, p.S10-S11), thereby producing  $\mathbf{H}(re)$  and  $\mathbf{H}(si)$ . The corresponding details for complexes for (R,R)-MeO-BIBOP ligand are shown in Figure 10 **A** (in **CSI**, Figure S8 and Table S3, p.S10-S12).

Energy profile diagram for the [(R,R)-BenzP\*[Co]+-me**diated reactions.** In our calculations using the (R,R)-BenzP\* ligand and a prototypical 2,4-disubstituted 1,3-diene, (E)-2methylpenta-1,3-diene, we found that the Oxidative Boryl Migration (Figure 7 C) is more feasible, as the transition state for the turn-over limiting steps leading to the major product, 4,3-HB,  $(TS_{III}(re) = 13.8 \text{ kcal/mol}$ , Figure 9) is characterized by the lowest energy among all of the other possible routes. See also CSI Figure S13 p. S30 for energy values with suitably larger basis sets. By comparison, no low-energy path was identified for the formation of the [4,3]-product in the Oxidative Hydrogen Migration route [CSI Figure S10, p.S13-S16 versus Figure S11. See also CSI Figure S12 (p. S17) for a side-by-side energy comparison of **OBM** and **OHM** routes. The lowest energy transition state for **OHM** is  $TS_{IX}(re)$  (= 18.3 kcal/mol), which should lead to a rarely seen [1,4]-HB product (See CSI Figure S12, for comparative energies of the various transition states involved in the OBM and the OHM routes with (R,R)-BenzP\* as ligand). A difference of 4.5 kcal/mol (marked  $\Delta\Delta G^{\ddagger}_{OBM}$  in CSI Figure S12) in favor of the Oxidative Boryl Migration over Oxidative Hydrogen Migration suggests that **OBM** is the most likely pathway for the hydroboration reaction. Use of different density functionals and basis sets (See CSI Table S4, p. S18) does not change this conclusion. Befittingly, we have used OBM pathway for all productive steps in the mechanism.

Thus, for the steps beyond the initial diastereoselective recognition of re-face of the 2,4-disubstituted diene by the  $[[(R,R)-BenzP^*]Co]^+$ , we proceeded further with the *Oxidative Boryl Migration* route. The *Oxidative Boryl Migration* to  $C_4$  is energetically more facile than migration to  $C_1$ , as corroborated by the Gibbs free energy of the corresponding transition states  $(TS_{III}(re) = 13.8 \text{ kcal/mol for } C_4\text{-borylation};$   $TS_{IV}(si) = 21.2 \text{ kcal/mol for } C_1\text{-borylation};$  Figure 9 B). We considered  $TS_{IV}(si)$  to be in the main operative pathway for 1,2-product formation since the  $TS_{IV}(re)$  is slightly higher energy than  $TS_{IV}(si)$  [22.3 kcal/mol and 21.2 kcal/mol for  $TS_{IV}(re)$  and  $TS_{IV}(si)$  respectively]. Therefore, the propensity of borylation at  $C_4(re)$  is favored by 7.4 kcal/mol energy (i.e., 21.2–13.8) difference (marked as  $\Delta\Delta G^{\ddagger}_4$  in Figure 9B) over the preferred pathway for  $C_1(si)$ -borylation.

As shown in Figure S13 in the **CSI** (p. S30), this value remains remarkably close to the values obtained from use of other different density functionals and basis sets – all  $\Delta\Delta G^{\ddagger}_4$  in the range of 7.4 to 7.7 kcal/mol (with energies of all TS's and intermediates being shown in **CSI** Tables S5, and S6, p. S18-S29). These calculations concurred with the experimental finding of [4,3]-HB being the major product, even though they do overestimate the energy differences. All of the important transition states for the hydroboration with ligand (R,R)-BenzP\* via **OBM** and **OHM** as calculated at the B3LYP-D3/6-31+G\*\* (SDD for cobalt) level of theory in the gas phase are shown in the **CSI** Figure S10-S12, p. S14-17. The key energy differences ( $\Delta\Delta G^{\ddagger}$ ) computed at various levels of theory are shown in **CSI** Table S4 (p. S18).

These calculations concurred with the experimental finding of [4,3]-HB being the major product, even though these gas phase calculations do overestimate the energy difference. Important transition states for the hydroboration with ligand (*R*,*R*)-BenzP\* via **OBM** and **OHM** as calculated at the B3LYP-D3/6-31+G\*\* (SDD for cobalt) level of theory in the gas phase are shown in the **CSI** Table S5, p.S18-S25.

Returning to the question of enantioselectivity in the major product, the relevant transition states in Figure 9 are TS<sub>III</sub>(re) (13.8 kcal/mol) and TS<sub>III</sub>(si) (23.3 kcal/mol). Clearly the difference in the free energies (9.5 kcal/mol, marked  $\Delta\Delta G^{\ddagger}_{ee}$ ) of these two transition states do suggest a strong preference for the formation of the  $\mathbf{III}(re)$  intermediate with (R)-configuration at C<sub>4</sub> over **III(si)** with (S)-configuration at C<sub>4</sub> (Figure 9 **B**). This is in complete agreement with the observed ee >99:1 for the ultimate [4,3]-hydroboration product of the diene when (R,R)-BenzP\* is used as the ligand. As for the next steps in the formation of the product V(re) from the  $\eta^3$ -allyl-cobalt species III(re), the calculations identified an energetically favorable conformational change to give III'(re) before the reductive elimination to form the C-H bond (see CSI Table S5 and Table S6, p. S19-S25) for structures and energies of this and related conformational isomers of these intermediates). This duly formed III'(re) intermediate can undergo reductive elimination at C<sub>3</sub> to give the alkene complex V(re) (Figure 9 **B**) of the final [4,3]-HB product **31b** (in Figure 8) via **TS**<sub>V</sub>(*re*) [9.0 kcal/mol]. The intermediate **III(re)** can, in principle, also undergo reductive elimination with C<sub>1</sub>-H bond formation via  $TS_{VI}(re)$  [13.6 kcal/mol] to form VI(re), the alkene complex of the [4,1]-HB product [= 31c in Figure 8]. Significant energy difference (4.6 kcal/mol, marked as  $\Delta\Delta G^{\dagger}_{4,3}$  in Figure 9 B) between  $TS_V(re)$  and  $TS_{VI}(re)$  precludes the formation of the [4,1]-HB-adduct. Experimentally also only the [4,3]-hydroboration-adduct is observed. We computed

intermediates and transition states of other probable pathways ([1,2]- and [1,4]-pathways) and unsurprisingly they were discarded as they were preceded by more energy-demanding transition states in the turn-over limiting step (first step, i.e.,

oxidative borylation) as compared to the transition state [TS<sub>III</sub>(re)] leading to the [4,3]-hydroboration (CSI, Figure S10, Figure S11; CSI p. S14-16 and CSI Table S5 and Table S6, p. S18 -S29).

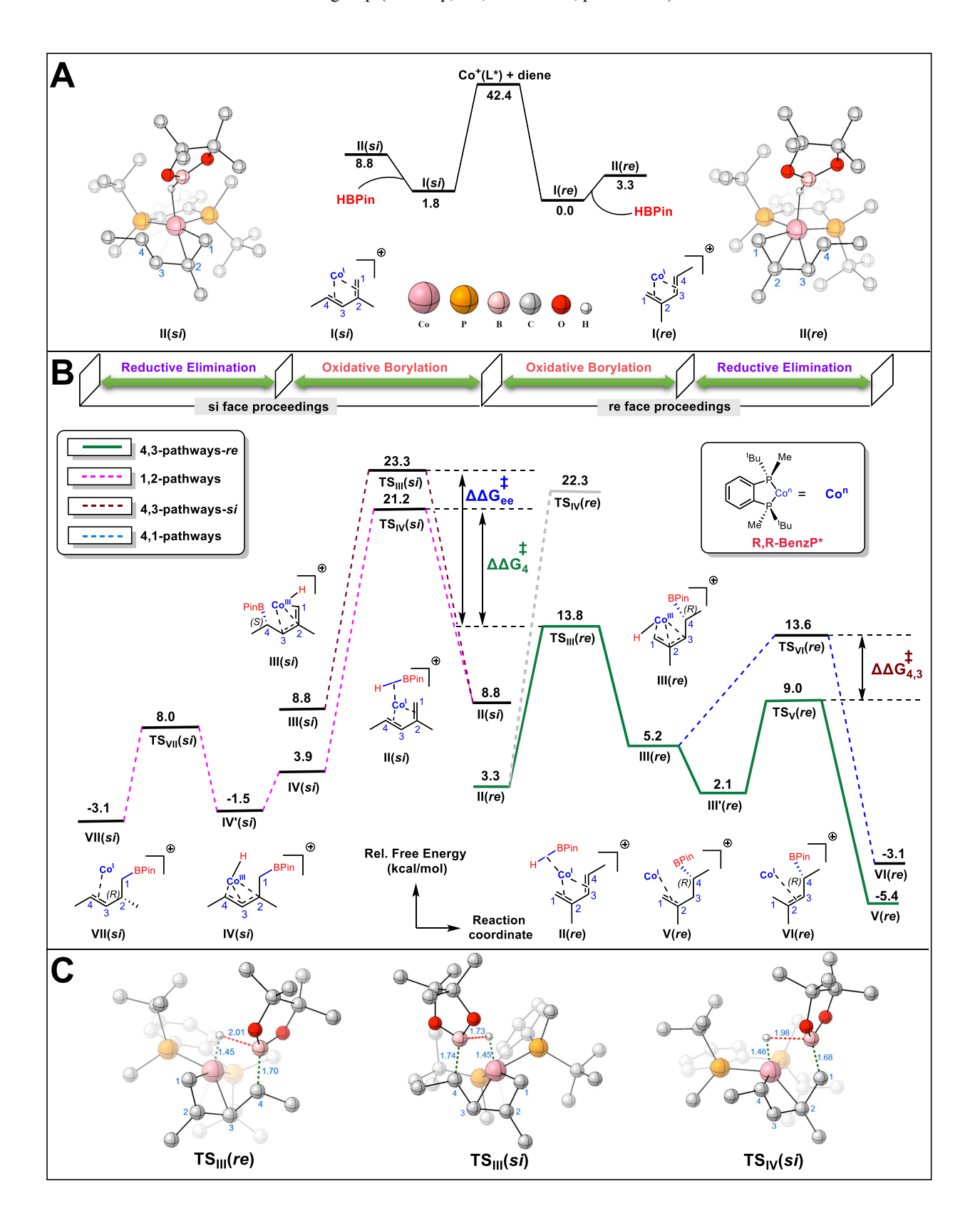
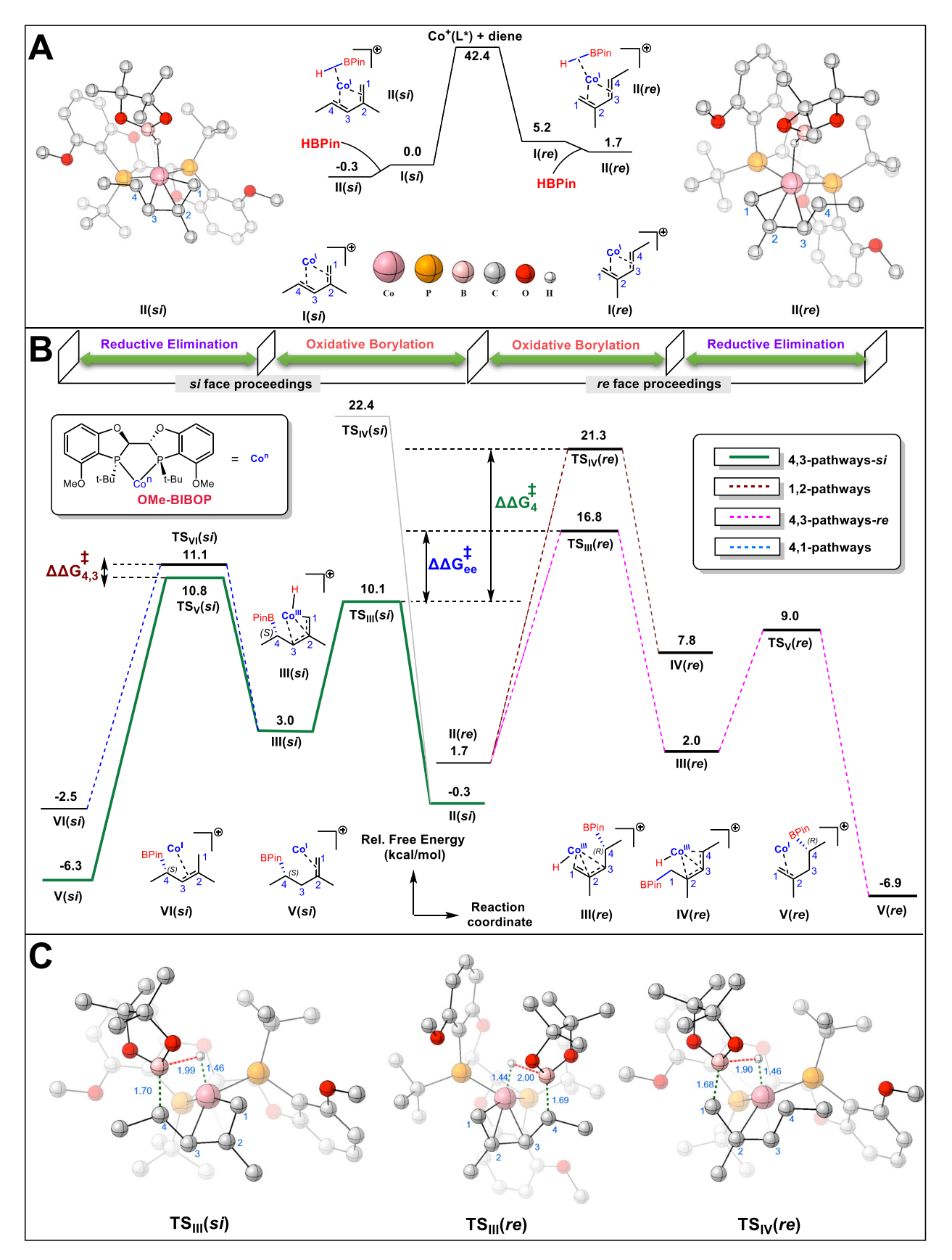


Figure 9. Stepwise events of Oxidative Boryl Migration of (E)-4-methyl-pentadiene with (R,R)-BenzP\* via re and si face binding calculated in gas phase, B3LYP-D3/6-31+G\*\*, SDD(Co), see also Figure S13 in the CSI (p. S30) for effect of different TZ basis sets including solvation. (A) Prochiral face recognition of the diene by the chiral (R,R)-BenzP\* ligand (I(re) and I(si)) and their HBPin adduct (II(re) and II(si)). (B) Origin of regio- and enantioselectivity in the formation of the 4,3-product as the major product over the [1,2]-product (Gibbs free energy as the Y-axis, and reaction coordinate as the X-axis). (C) Three important transition states pertinent to explain the regioselectivity of the [4,3] over [1,2]-product (TS<sub>III</sub>(re) vs TS<sub>III</sub>(si)) and high enantioselectivity of the [4,3]-product (TS<sub>III</sub>(re) vs TS<sub>III</sub>(si)), for rest of the transition states and intermediates see CSI, Figure S10, p. S14 and Table S5-S6, p. S18-29. Energies that correspond to the regioselectivities are designated as  $\Delta\Delta$ G<sup>‡</sup><sub>4</sub>: for 4,3- vs 1,2- and  $\Delta\Delta$ G<sup>‡</sup><sub>4,3</sub> for 4,3- vs 4,1; Similarly, energy that indicates enantioselectivity is marked as  $\Delta\Delta$ G <sup>‡</sup><sub>ee</sub>: C4(R) vs C4(S).

Energy profile diagram for the [[(R,R)-OMe-BIBOP]Co]+mediated reactions. Contrary to what was observed with (R,R)-BenzP\*, the si-face diastereomeric adduct of the 2,4-disubstituted diene with the [(R,R)-MeO-BIBOP(Co)]<sup>+</sup> complex was favored (Figure 10 A, in CSI: Figure S6 and Table S2, p. S8-S9). Nevertheless, the reaction proceeds through the Oxidative Boryl Migration route (see CSI for the corresponding energy profiles, **CSI**: Figures S14 - Figure S16, p. S31-S33). The initial binding of HBPin (Figure 10 A, see also CSI: Table S3, Figure S8, CSI p.S10-S12) to the si-face-bound diene would lead to Oxidative Boryl Migration to C<sub>4</sub> via TS<sub>III</sub>(si) in the first step of the **OBM** pathway with a free energy of 10.1 kcal/mol (Figure 10 B). The  $TS_{IV}(re)$  [21.3 kcal/mol] is slightly favored over TS<sub>IV</sub>(si) [22.4 kcal/mol] for a pathway that corresponds to [1,2]-hydroboration product formation. The large proclivity for boryl migration to the 4-position (vs 1-position) of the diene is the result of a  $\Delta\Delta G^{\ddagger}_{4} = 11.2$ kcal/mol (21.3 –10.1) (Figure 10 **B**), more than sufficient to explain the astounding regioselectivity (4.1- vs 1.2) of 98:1 with the ligand (R,R)-MeO-BIBOP. While the predicted change in energy of the transition states was larger than expected, this correlated well with the experimental results.



**Figure 10.** Stepwise events of *Oxidative Boryl Migration* of (*E*)-4-imethyl-pentadiene with (*R*,*R*)-MeO-BIBOP via *re* and *si* face binding, calculated in gas phase, B3LYP-D3/6-31+G\*\*, SDD(Co), see also Figure S17 in the **CSI** (p. S44) for effect of different basis sets including solvation. (**A**) Prochiral face recognition of the diene by the chiral (*R*,*R*)- MeO-BIBOP ligand (**I**(*re*) and **I**(*si*)) and their HBPin adduct (**II**(*re*) and **II**(*si*)). (**B**) Origin of regio- and enantioselectivity in forming the [4,3]-product as the major product over the [1,2]-product via the *si* face (Gibbs free energy on the Y-axis, reaction coordinate as the X-axis). (**C**) Three important transition states germane to the regioselectivity of

[4,3]- over [1,2]- product [( $\mathbf{TS}_{III}(si)$ ) vs  $\mathbf{TS}_{IV}(re)$ ] and high enantioselectivity in the [4,3]-product [( $\mathbf{TS}_{III}(si)$ ) vs  $\mathbf{TS}_{III}(re)$ ]. For rest of the transition states and intermediates refer to  $\mathbf{CSI}$ , Figure S14, p. S31, and Table S8-S9, p. S34-S43. Energies that signify regioselectivities are designated as  $\Delta\Delta\mathbf{G}^{\ddagger}_{4}$ : for 4,3- vs 1,2- and  $\Delta\Delta\mathbf{G}^{\ddagger}_{4,3}$  for 4,3- vs 4,1; Likewise, energy differences for enantioselectivity is marked as  $\Delta\Delta\mathbf{G}^{\ddagger}_{ee}$ : C4(S) vs C4(R).

For the assessment of the enantioselectivity with the (R,R)-MeO-BIBOP ligand, the preference for TS<sub>III</sub>(si) vs TS<sub>III</sub>(re) is by 6.7 kcal/mol, marked  $\Delta \Delta G^{\ddagger}_{ee}$ , Figure 10 **B**. This result is in accord with the experimentally observed (S)-configuration at C<sub>4</sub>. As a result, we suggest a strong preference for the formation of the III(si) from  $TS_{III}(si)$  over III(re) from  $TS_{III}(re)$ which results in >99:1 er. Furthermore, from the newly formed cobalt-hydride  $\eta^3$ -allyl species [III(si)], we sought to predict the formation of possible V(si) and VI(si) products corresponding to [4,3]-hydroboration and [4,1]-hydroboration products, respectively. Contrary to (R,R)-BenzP\*, no appreciable molecular reorganization from III(si) was observed before the final reductive elimination step (see CSI Table S9, p. S40-S43). TS<sub>V</sub>(si) was predicted to be the most facile at a relative TS free energy of 10.8 kcal/mol leading to the desired [4,3]-hydroboration product [V(si)]. However, the transition state for the formation of a [4,1]-product  $[TS_{VI}(si)]$  seemed to be nearly equally probable at a relative free energy of 11.1 kcal/mol (difference of just 0.3 kcal/mol, marked as  $\Delta\Delta G^{\dagger}_{4,3}$ in Figure 10 B). While this was an unexpected computational result, equally unexpected was the remarkable solvent effect that was observed in this [(R,R)-MeO-BIBOP(Co)]<sup>+</sup>catalyzed reaction and how easily the [4,3]-HB product is converted into the [4,1]-adduct (Figure 4, B and C) While the [4,3]-adduct was observed experimentally in diethyl ether as a solvent, in a non-coordinating solvent like DCM, the major

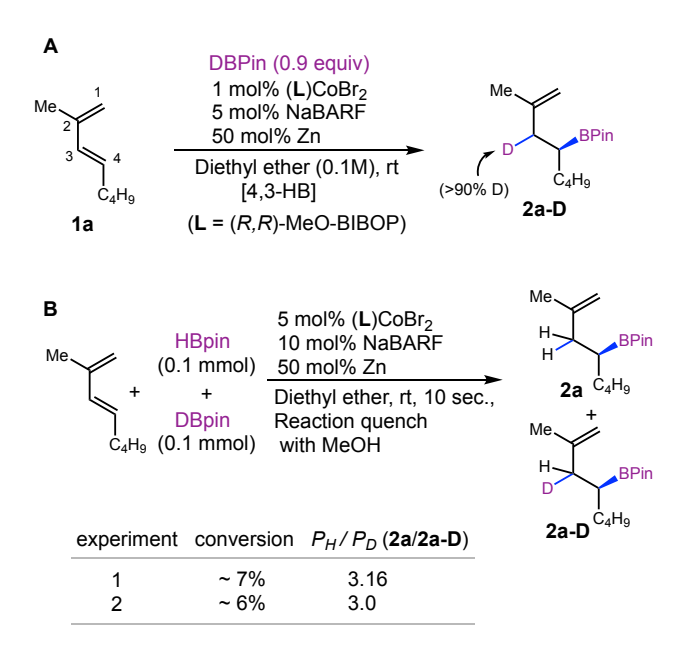


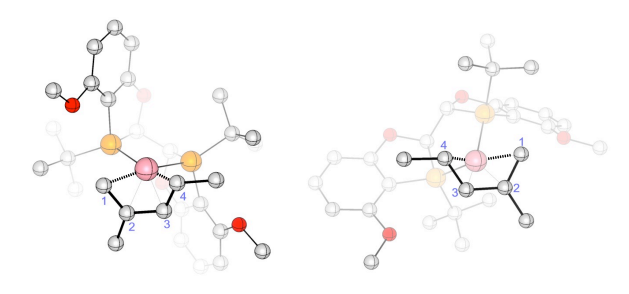
**Figure 11.** Isotopic labeling studies. **A.** Addition of DBPin to **1a** gives the expected 4,3-HB-product **2a-D. B.** Intermolecular competition experiment with a significant kinetic isotope effect is consistent with the oxidative boryl migration proposed as s key step in the mechanism (see Figure 7 **C**).

product was the more stable [4,1]-hydroboration product. The ambiguity of the distribution of [4,3]- vs [4,1]-product with (R,R)-MeO-BIBOP with changing solvents should invite caution in choosing a solvent for optimum selectivity in these reactions. Indeed, we have shown experimentally that the [4,3]-product undergoes facile isomerization to the [4,1]-product under the reaction conditions in CH<sub>2</sub>Cl<sub>2</sub> (Figure 4, C) Incidentally, calculations with SMD(diethyl ether)/B3LYP-D3/def2TZVP, SDD(Co) produced a larger  $\Delta\Delta G^{\ddagger}_{4,3}$  ( $\sim 1.0$  kcal/mol) [Figure S17, p. S44) as compared to gas phase difference in free energies (0.3 kcal/mol).

Isotope labeling studies. Detailed kinetic studies of the reaction is beyond the scope of the current investigations, partly because we find that the initial rates to be too fast to permit standard techniques. However, we have carried out isotope labeling studies using DBPin, and the results are shown in Figure 11. Use of DBPin gives the expected 4,3-adduct with incorporation of >85% D at the C<sub>3</sub> position (see Supporting Information (Experimental) for details, P. S42-S45. Intermolecular competition experiment with excess 1,3-diene and 1 equivalent each of HBPin and DBPin gives non-deuterated and mono-deuterated 2a in a ratio of ~3 (reaction done in duplicate), presumably showing a primary kinetic isotope effect. This experiment is consistent with the Oxidative Boryl Migration to the diene C4 with B-H cleavage, proposed as the ratelimiting step in the mechanism (see Figure 8 C), even though it does not altogether rule out alternate mechanistic possibilities.

### **CONCLUSIONS**

Among α-stereogenic organoboranes, enantiopure homoallylic boronates, carrying multiple latent functionalities are the most versatile, and their synthesis has attracted considerable attention. Yet, one of the most direct approaches to these compounds, viz., regio- and enantioselective hydroboration of readily available 1,3-dienes has remained an unmet challenge. We have identified reaction conditions and ligands for the synthesis of nearly enantiopure (er >99:1 to >97:3) homoallyl boronates via a rarely seen cobalt-catalyzed [4,3]-hydroboration of 1,3-dienes. Monosubstituted or 2,4-disubstituted linear dienes undergo highly efficient, regio- and enantioselective hydroboration with HBPin catalyzed [(L\*)Co]<sup>+</sup>[BARF]<sup>-</sup>, where L\* is typically a chiral bis-phosphine ligand with a narrow bite angle. While a number of such ligands (for example, i-PrDuPhos, QuinoxP\*, Duanphos and, BenzP\*) gave very high enantioselectivities for the [4,3]hydroboration product, the equally challenging problem of regioselectivity is uniquely solved with a benzooxaphosphole ligand, MeO-BIBOP. A cationic cobalt(I) complex of this ligand is a very efficient (TON >960) catalyst, while providing excellent regioselectivities and enantioselectivities for a broad range of substrates including those carrying enol silanes, enol acetates, -OH, -OMs, -N<sub>3</sub>, -OTBS, vinyl as well as sensitive aromatic and heteroaromatic groups.



I(re) 5.2 kcal/mol

I(si) 0.0 kcal/mol

**Figure 12.** Diastereomers of [(R,R)-MeO-BIBOP]Co(diene)]<sup>+</sup> complexes showing relative energies (see also Figure 10). The product of enantioselective hydroboration (er >99:1) correspond to C<sub>4</sub> incorporation of boron via the complex I(si). Initial relative stabilities of diastereomeric complexes dictate the regio- and enantioselectivities.

Detailed computational investigation of the reactions provides results that are in good agreement with the experimental observations, and we are able to predict and rationalize the regio- and enantioselectivity of hydroboration with bis-phosphine ligands. Difference in ground state stabilization of diene-bound cobalt complex leads to facial selectivity, which in turn is carried through the subsequent steps (Figures 10 and 12). There is no indication of any low-energy routes that proceed through the less stable initial diastereomeric  $[(L)Co(diene)]^+$  complex [I(si) in the case of (R,R)-BenzP\* ligand, or, the complex I(re) in the case of [(R,R)-MeO-BIBOP ligand], being involved. This reaction is unlikely to be complicated by Curtin-Hammett kinetics, at least with catalysts we have studied thus far. Thus it may be possible to predict the configuration of the final products based on the energy differences in the diastereomers of the initially formed [(L\*)Co<sup>I</sup>(diene)]<sup>+</sup> complexes. We are currently seeking validation for these ideas through further experimental work, including isolation and identification of the relevant diastereomeric complexes and the products derived from them using structurally different ligands.

### ASSOCIATED CONTENT

### **Supporting Information**

The Supporting Information is available free of charge on the ACS Publication website at DOI: 10.1021/jacs.xxxxxxx.

**Supporting Information (Experimental)** contains full experimental details for the preparation of all new compounds, and their spectroscopic and chromatographic data including Chiral Stationary Phase GC or HPLC separations showing enantiomeric ratios. Tables with details of optimization studies, Figure showing names, structures and sources of all chiral ligands. Crystallographic Data for the complexes, [(1R,2S)-Daunphos]CoBr<sub>2</sub>, [(R,R)-MeO-BIBOP]CoBr<sub>2</sub>. These structures have been deposited at Cambridge Crystal Data Centre and have the following numbers: 2151424, 2151425 respectively.

Supporting Information for Computational Part (CSI) contains details of various plausible mechanisms of Co-catalyzed hydroboration, details of the geometries and energies of all relevant intermediates and the corresponding transition states calculated at the B3LYP-D3/6-31+G\*\* (SDD for cobalt) level of theory in

the gas phase. Results of single point energy calculations to explore solvation effects, different functional and basis sets such as 6-311+G\*\*TZ. XYZ coordinates of all atoms in relevant intermediates and transition states.

Supporting Information Part I (Experimental).pdf Supporting Information Part II (Computational).pdf

### **AUTHOR INFORMATION**

### **Corresponding Authors**

T. V. RajanBabu, Department of Chemistry and Biochemistry, The Ohio State University, Columbus, Ohio 43210, United States; orcid.org/0000-0001-8515-3740; Email: rajanbabu.1@osu.edu

Christopher M. Hadad, Department of Chemistry and Biochemistry, The Ohio State University, Columbus, Ohio 43210, United States; orcid.org/0000-0003-1211-4315; Email: hadad.1@osu.edu

### **Authors**

Mahesh M. Parsutkar orcid.org/0000-0001-6320-2345 Subhajit Bhunia Mayukh Majumder Remy F. Lalisse orcid.org/0000-0002-4556-5641

### **Author Contributions**

<sup>‡</sup> These authors contributed equally.

### **Funding Sources**

U.S. National Institutes of Health (1 R35 GM139545-01) and the U.S. National Science Foundation (CHE-1900141).

### Notes

The authors declare no competing financial interest.

### **ACKNOWLEDGMENTS**

We like to thank Dr. Curtis Moore for the determination of the solid-state structures by X-ray crystallography. Financial assistance for this research provided by the U.S. National Institutes of Health (1 R35 GM139545-01) and the U.S. National Science Foundation (CHE-1900141) is gratefully acknowledged. MMP is grateful for an Ohio State University Presidential Fellowship. We thank Professor David Nagib for the use of a CSP HPLC. MM and RFL gratefully acknowledge generous computational resources provided by the Ohio Supercomputer Center. MM thanks Biswajit Biswas for valuable discussions.

### REFERENCES

1. (a) For a recent review, see: Hu, J.; Ferger, M.; Shi, Z.; Marder, T. B. Recent advances in asymmetric borylation by transition metal catalysis. *Chem. Soc. Rev.* **2021**, *50*, 13129-13188. For representative examples illustrating various methods, see: (b) Namirembe, S.; Morken, J. P. Reactions of organoboron compounds enabled by catalyst-promoted metalate shifts. *Chem. Soc. Rev.* **2019**, *48*, 3464-3474. (c) Chen, J. B.; Whiting, A. Recent Advances in Copper-Catalyzed Asymmetric Hydroboration of Electron-Deficient Alkenes: Methodologies and Mechanism. *Synthesis-Stuttgart* **2018**,

- 50, 3843-3861. (d) Hall, D. G.; Lee, J. C. H.; Ding, J. Y. Catalytic enantioselective transformations of borylated substrates: Preparation and synthetic applications of chiral alkylboronates. *Pure Appl. Chem.* **2012**, 84, 2263-2277. (e) Sandford, C.; Aggarwal, V. K. Stereospecific functionalizations and transformations of secondary and tertiary boronic esters. *Chem. Commun.* **2017**, 53, 5481-5494. (f) Xu, N.; Liang, H.; Morken, J. P. Copper-Catalyzed Stereospecific Transformations of Alkylboronic Esters. *J. Am. Chem. Soc.* **2022**, 144, 11546-11552. (g) Matteson, D. S. α-Halo boronic esters: intermediates for stereodirected synthesis. *Chem. Rev.* **1989**, 89, 1535-1551. (h) Brown, H. C.; Singaram, B. Development of a simple general procedure for synthesis of pure enantiomers via chiral organoboranes. *Acc. Chem. Res.* **1988**, 21, 287-293.
- (a) Collins, B. S. L.; Wilson, C. M.; Myers, E. L.; Aggarwal, V. K. Asymmetric Synthesis of Secondary and Tertiary Boronic Esters. Angew. Chem. Int. Ed. 2017, 56, 11700-11733. (b) For another novel approach to these compounds that involve boronate esters see: Zhang, C.; Hu, W.; Lovinger, G. J.; Jin, J.; Chen, J.; Morken, J. P. Enantiomerically Enriched α-Borylzinc Reagents by Nickel-Catalyzed Carbozincation of Vinylboronic Esters. J. Am. Chem. Soc. 2021, 143, 14189-14195. (c) Kubota, K.; Miura, D.; Takeuchi, T.; Osaki, S.; Ito, H. Synthesis of Chiral α-Amino Tertiary Boronates via the Catalytic Enantioselective Nucleophilic Borylation of Dialkyl Ketimines. ACS Catal. 2021, 11, 6733-6740. (d) Gao. D. W.; Gao, Y.; Shao, H. L.; Qiao, T. Z.; Wang, X.; Sanchez, B. B.; Chen, J. S.; Liu, P.; Engle, K. M. Cascade CuH-catalysed conversion of alkynes into enantioenriched 1,1-disubstituted products. Nature Catal. 2020, 3, 23-29. (e) Sardini, S. R.; Lambright, A. L.; Trammel, G. L.; Omer, H. M.; Liu, P.; Brown, M. K. Ni-Catalyzed Arylboration of Unactivated Alkenes: Scope and Mechanistic Studies. J. Am. Chem. Soc. 2019, 141, 9391-9400. (f) Gao, T. T.; Zhang, W. W.; Sun, X.; Lu, H. X.; Lio, B. J. Stereodivergent Synthesis through Catalytic Asymmetric Reversed Hydroboration. J. Am. Chem. Soc. 2019, 141, 4670-4677. (g) Chen, X.; Cheng, Z. Y.; Guo, J.; Lu, Z. Asymmetric remote C-H borylation of internal alkenes via alkene isomerization. Nature Commun. 2018, 9, 3939. (h) Pang, Y.; He, Q.; Li, Z. Q.; Yang, J. M.; Yu, J. H.; Zhu, S. F.; Zhou, Q. L. Rhodium-Catalyzed B-H Bond Insertion Reactions of Unstabilized Diazo Compounds Generated in Situ from Tosylhydrazones. J. Am. Chem. Soc. 2018, 140, 10663-10668. (i) Lee, J.; Torker, S.; Hoveyda, A. H. Versatile Homoallylic Boronates by Chemo-,  $S_{N2}$ '-, Diastereo- and Enantioselective Catalytic Sequence of Cu-H Addition to Vinyl-B(pin)/Allylic Substitution. Angew. Chem. Int. Ed. 2017, 56, 821-826. (j) Zhang, L.; Lovinger, G. J.; Edelstein, E. K.; Szymaniak, A. A.; Chierchia, M. P.; Morken, J. P. Catalytic conjunctive crosscoupling enabled by metal-induced metallate rearrangement. Science 2016, 351, 70-74. (k) Schmidt, J.; Choi, J.; Liu, A. T.; Slusarczyk, M.; Fu, G. C. A general, modular method for the catalytic asymmetric synthesis of alkylboronate esters. Science 2016, 354, 1265-1269. (1) Kubota, K.; Watanabe, Y.; Hayama, K.; Ito, H. Enantioselective Synthesis of Chiral Piperidines via the Stepwise Dearomatization/Borylation of Pyridines. J. Am. Chem. Soc. 2016, 138, 4338-4341. (m) Lee, J. C. H.; Hall, D. G. Chiral Boronate Derivatives via Catalytic Enantioselective Conjugate Addition of Grignard Reagents on 3-Boronyl Unsaturated Esters and Thioesters. J. Am. Chem. Soc. 2010, 132, 5544-5545.
- 3. (a) For a recent review see, Zuo, Z. Q.; Wen, H. N.; Liu, G. X.; Huang, Z. Cobalt-Catalyzed Hydroboration and Borylation of Alkenes and Alkynes, *Synlett* **2018**, *29*, 1421-1429. For recent examples of enantioselctive hydroboration of alkenes, see: (b) Bai, X.-Y.; Zhao, W.; Sun, X.; Li, B.-J. Rhodium-Catalyzed Regiodivergent and Enantioselective Hydroboration of Enamides. *J. Am. Chem. Soc.* **2019**, *141*, 19870-19878. (c) Chen, X.; Cheng, Z.; Lu, Z. Cobalt-Catalyzed Asymmetric Markovnikov Hydroboration of Styrenes. *ACS Catal.* **2019**, *9*, 4025-4029. (d) Teo, W. J.; Ge, S. Z. Cobalt-Catalyzed Enantioselective Synthesis of Chiral *gem*-Bis(boryl)alkanes. *Angew. Chem. Int. Ed.* **2018**, *57*, 12935-12939. (e) Wen, L.; Cheng, F. C.; Li, H.; Zhang, S. Q.; Hong, X.; Meng, F. K. Copper-Catalyzed Enantioselective Hydroboration of 1,1-Disubstituted Alkenes: Method Development, Applications and Mechanistic Studies, *Asian J. Org. Chem.* **2018**, *7*, 103-106. (f) Cai,

- Y.; Yang, X. T.; Zhang, S. Q.; Li, F.; Li, Y. Q.; Ruan, L. X.; Hong, X.; Shi, S. L. Copper-Catalyzed Enantioselective Markovnikov Protoboration of alpha-Olefins Enabled by a Buttressed N-Heterocyclic Carbene Ligand, Angew. Chem. Int. Ed. 2018, 57, 1376-1380. (g) Xi, Y. M.; Hartwig, J. F. Diverse Asymmetric Hydrofunctionalization of Aliphatic Internal Alkenes through Catalytic Regioselective Hydroboration. J. Am. Chem. Soc. 2016, 138, 6703-6706. (h) Jang, W. J.; Song, S. M.; Moon, J. H.; Lee, J. Y.; Yun, J. Copper-Catalyzed Enantioselective Hydroboration of Unactivated 1,1-Disubstituted Alkenes, J. Am. Chem. Soc. 2017, 139, 13660-13663. (i) Smith, J. R.; Collins, B. S. L.; Hesse, M. J.; Graham, M. A.; Myers, E. L.; Aggarwal, V. K. Enantioselective Rhodium(III)-Catalyzed Markovnikov Hydroboration Unactivated Terminal Alkenes. J. Am. Chem. Soc. 2017, 139, 9148-9151. (j) Zhang, L.; Zuo, Z.; Wan, X.; Huang, Z. Cobalt-Catalyzed Enantioselective Hydroboration of 1,1-Disubstituted Aryl Alkenes, J. Am. Chem. Soc. 2014, 136, 15501-15504. (k) Corberán, R.; Mszar, N. W.; Hoveyda, A. H. NHC-Cu-Catalyzed Enantioselective Hydroboration of Acyclic and Exocyclic 1,1-Disubstituted Aryl Alkenes, Angew. Chem. Int. Ed. 2011, 50, 7079-7082. (1) Mazet, C.; Gérard, D. Highly regio- and enantioselective catalytic asymmetric hydroboration of α-substituted styrenyl derivatives, *Chem. Commun*. 2011, 47, 298-300. (m) Hayashi, T.; Matsumoto, Y.; Ito, Y. Asymmetric hydroboration of styrenes catalyzed by cationic chiral phosphine-rhodium(I) complexes, Tetrahedron: Asymmetry 1991, 2, 601-612.
- 4. (a) Perry, G. J. P.; Jia, T.; Procter, D. J. Copper-catalyzed functionalization of 1,3-dienes: Hydrofunctionalization, borofunctionalization, and difunctionalization. *ACS Catal.* **2020**, *10*, 1485-1499. (b) Li, G. L.; Huo, X. H.; Jiang, X. Y.; Zhang, W. B. Asymmetric synthesis of allylic compounds via hydrofunctionalisation and difunctionalisation of dienes, allenes, and alkynes. *Chem. Soc. Rev.* **2020**, *49*, 2060-2118.
- 5. In this paper the regioselectivity of hydroboration using pinacol borane (H–X = H–BPin) is defined by the numbers of the carbons on the diene to which are linked B and H, respectively. For the sake of consistency in numbering across various dienes used in this study, the diene is always labeled with the terminal unsubstituted = $CH_2$  as  $C_1$  (see Figure 1 B).
- (a) Kim, I. S.; Ngai, M.-Y.; Krische, M. J. Enantioselective Iridium-Catalyzed Carbonyl Allylation from the Alcohol or Aldehyde Oxidation Level via Transfer Hydrogenative Coupling of Allyl Acetate: Departure from Chirally Modified Allyl Metal Reagents in Carbonyl Addition. J. Am. Chem. Soc. 2008, 130, 14891-14899. (b) Holmes, M.; Schwartz, L. A.; Krische, M. J. Intermolecular Metal-Catalyzed Reductive Coupling of Dienes, Allenes, and Enynes with Carbonyl Compounds and Imines. Chem. Rev. 2018, 118, 6026-6052. (c) Keck, G. E.; Tarbet, K. H.; Geraci, L. S. Catalytic asymmetric allylation of aldehydes. J. Am. Chem. Soc. 1993, 115, 8467-8468. (d) Denmark, S. E.; Fu, J. P. Catalytic, enantioselective addition of substituted allylic trichlorosilanes using a rationally-designed 2,2'-bispyrrolidine-based bisphosphoramide. J. Am. Chem. Soc. 2001, 123, 9488-9489. Stoichiometric methods: (e) Brown, H. C.; Jadhav, P. K. Asymmetric carbon carbon bond formation via beta-allyldiisopinocampheylborane - simple synthesis of secondary homoallylic alcohols with excellent enantiomeric purities. J. Am. Chem. Soc. 1983, 105, 2092-2093. (f) Roush, W. R.; Walts, A. E.; Hoong, L. K. Diastereoselective and enantioselective aldehyde addition-reactions of 2-allyl-1,3,2-dioxaborolane-4,5-dicarboxylic esters, a useful class of tartrate ester modified allylboronates. J. Am. Chem. Soc. 1985, 107, 8186-8190. (g) Kinnaird, J. W. A.; Ng, P. Y.; Kubota, K.; Wang, X. L.; Leighton, J. L. Strained silacycles in organic synthesis: A new reagent for the enantioselective allylation of aldehydes. J. Am. Chem. Soc. 2002, 124, 7920-7921. (h) A review of catalytic Nozaki-Hiyama-Kishi coupling: Hargaden, G. C.; Guiry, P. J. Adv. Synth. Catal. 2007, 349, 2407.
- 7. Boiarska, Z.; Braga, T.; Silvani, A.; Passarella, D. Brown Allylation: Application to the Synthesis of Natural Products. *Eur. J. Org. Chm.* **2021**, *2021*, 3214-3222.
- 8. (a) Ibrahim, A. D.; Entsminger, S. W.; Fout, A. R. Insights into a Chemoselective Cobalt Catalyst for the Hydroboration of

- Alkenes and Nitriles. ACS Catal. 2017, 7, 3730-3734. (b) Semba, K.; Shinomiya, M.; Fujihara, T.; Terao, J.; Tsuji, Y. Highly Selective Copper-Catalyzed Hydroboration of Allenes and 1,3-Dienes. Chem. Eur. J. 2013, 19, 7125-7132. (c) Obligacion, J. V.; Chirik, P. J. Bis(imino)pyridine Cobalt-Catalyzed Alkene Isomerization-Hydroboration: A Strategy for Remote Hydrofunctionalization with Terminal Selectivity. J. Am. Chem. Soc. 2013, 135, 19107-19110. (d) Wu, J. Y.; Moreau, B.; Ritter, T. Iron-Catalyzed 1,4-Hydroboration of 1,3-Dienes. J. Am. Chem. Soc. 2009, 131, 12915-12917. (e) Ely, R. J.; Morken, J. P. Regio- and Stereoselective Ni-Catalyzed 1,4-Hydroboration of 1,3-Dienes: Access to Stereodefined (Z)-Allylboron Reagents and Derived Allylic Alcohols. J. Am. Chem. Soc. 2010, 132, 2534-2535. (f) Sasaki, Y.; Zhong, C.; Sawamura, M.; Ito, H. Copper(I)-Catalyzed Asymmetric Monoborylation of 1,3-Dienes: Synthesis of Enantioenriched Cyclic Homoallyl- and Allylboronates. J. Am. Chem. Soc. 2010, 132, 1226-1227. (g) Zaidlewicz, M.; Meller, J. Syntheses with organoboranes. XII. Monohydroboration of conjugated dienes, alkynes and functionalized alkynes with catecholborane catalyzed by nickel(II) chloride and cobalt(II) chloride complexes with phosphines. Main Group Metal Chemistry 2000, 23, 765-772.
- 9. Liu, Y. B.; Fiorito, D.; Mazet, C. Copper-catalyzed enantioselective 1,2-borylation of 1,3-dienes. *Chem. Sci.* **2018**, *9*, 5284-5288.
- 10. Duvvuri, K.; Dewese, K. R.; Parsutkar, M. M.; Jing, S. M.; Mehta, M. M.; Gallucci, J. C.; RajanBabu, T. V. Cationic Co(I)-Intermediates for Hydrofunctionalization Reactions: Regio- and Enantioselective Cobalt-Catalyzed 1,2-Hydroboration of 1,3-Dienes. *J. Am. Chem. Soc.* **2019**, *141*, 7365-7375.
- 11. Cao, Y.; Zhang, Y.; Zhang, L.; Zhang, D.; Leng, X.; Huang, Z. Selective synthesis of secondary benzylic (*Z*)-allylboronates by Fe-catalyzed 1,4-hydroboration of 1-aryl-substituted 1,3-dienes. *Org. Chem. Front.* **2014**, *1*, 1101-1106.
- 12. (a) Parsutkar, M. Development of Cationic Cobalt(I)-Complexes for Enantioselective Cycloaddition and Hydrofunctionalization Reactions: From Readily Available Materials to Value-Added Products. PhD Dissertation, The Ohio State University, Columbus, OH, 2021. (b) Parsutkar, M. M.; Jing, S. M.; Duvvuri, K.; RajanBabu, T. V. In *Cationic cobalt(I) intermediates in hydrofunctionalization reactions*, 259th ACS National Meeting & Exposition, Philadelphia, PA, United States, March 22-26, 2020; American Chemical Society: Philadelphia, PA, United States, 2020; pp ORGN-0085.
- 13. Xu, R. S.; Rohde, L. N.; Diver, S. T. Regioselective Cu-Catalyzed Hydroboration of 1,3-Disubstituted-1,3-Dienes: Functionalization of Conjugated Dienes Readily Accessible through Ene-Yne Metathesis. *ACS Catal.* **2022**, *12*, 6434-6443.
- 14. (a) Jing, S. M.; Balasanthiran, V.; Pagar, V.; Gallucci, J. C.; RajanBabu, T. V. Catalytic Enantioselective Hetero-dimerization of Acrylates and 1,3-Dienes. *J. Am. Chem. Soc.* **2017**, *139*, 18034-18043. (b) New reduction procedures for synthesis of LCo(I)-complexes and comparison to in situ generated catalysts. Parsutkar, M. M.; Moore, C. E.; RajanBabu, T. V. Activator-free single-component Co(I)-catalysts for regio- and enantioselective heterodimerization and hydroacylation reactions of 1,3-dienes. *Dalton Trans.* **2022**, *51*, 10148-10159.
- 15. These angles were calculated from the solid-state structures of the respective LCoBr<sub>2</sub> complexes. See Suppoting Information for details including cif files for the new complexes. These structures (identified by L) have been deposited at CDCC. (1*R*,2*S*)-Duanphos CCDC # 2151424; (*R*,*R*,*R*,*R*)-MeO-BIBOP CCDC # 2151425. (*R*,*R*)-*i*-PrDuPhos CCDC # 2074145 (Parsutkar, M. M.; RajanBabu, T. V. alpha- and beta-Functionalized ketones from 1,3-dienes and aldehydes: Control of regio- and enantioselectivity in hydroacylation of 1,3-dienes. *J. Am. Chem. Soc.* 2021, 143, 12825-12835). (*S*,*S*)-BenzP\*-complex CCDC # 2151426 was recently published (Singh, D.: RajanBabu, T. V. Chemodivergent, Regio- and Enantioselective Cycloaddition Reactions between 1,3-Dienes and Alkynes. *Angew. Chem. Int. Ed.* 2023, e202216000. DOI: 10.1002/anie.202216000, in press.

- 16. Xu, G.; Senanayake, C. H.; Tang, W. *P*-Chiral Phosphorus Ligands Based on a 2,3-Dihydrobenzo[d][1,3]oxaphosphole Motif for Asymmetric Catalysis. *Acc. Chem. Res.* **2019**, *52*, 1101-1112.
- 17. (a) Dong, W.; Ye, Z.; Zhao, W., Enantioselective Cobalt-Catalyzed Hydroboration of Ketone-Derived Silyl Enol Ethers. *Angew. Chem. Int. Ed.* **2022**, *61*, e202117413. (b) Yu, S.; Wu, C.; Ge, S. Cobalt-Catalyzed Asymmetric Hydroboration/Cyclization of 1,6-Enynes with Pinacolborane. *J. Am. Chem. Soc.* **2017**, *139*, 6526-6529.
- 18. Kilner, M.; Parkin, G. Lithium nitride reduction of Cp<sub>2</sub>TiCl<sub>2</sub> and CpTiCl<sub>3</sub> the synthesis of (Cp<sub>2</sub>TiCl<sub>2</sub>, (CpTiCl<sub>2</sub>)<sub>n</sub>, Cp<sub>2</sub>Ti(CO)<sub>2</sub> and chlorotetratitanium and nitridohexatitanium complexes. *J. Organomet. Chem.* **1986**, *302*, 181-191.
- 19. Tsurugi, H.; Mashima, K. Salt-Free Reduction of Transition Metal Complexes by Bis(trimethylsilyl)cyclohexadiene, -dihydropyrazine, and -4,4'-bipyridinylidene Derivatives. *Acc. Chem. Res.* **2019**, *52*, 769-779.
- 20. Ishihara, K.; Mouri, M.; Gao, Q.; Maruyama, T.; Furuta, K.; Yamamoto, H. Catalytic asymmetric allylation using a chiral (acyloxy)borane complex as a versatile Lewis acid catalyst. *J. Am. Chem. Soc.* **1993**, *115*, 11490-11495.
- 21. Sabbani, S.; La Pensée, L.; Bacsa, J.; Hedenström, E.; O'Neill, P. M. Diastereoselective schenck ene reaction of singlet oxygen with chiral allylic alcohols; access to enantiomerically enriched 1,2,4-trioxanes. *Tetrahedron* **2009**, *65*, 8531-8537.
- 22. Rawal, V. H.; Kozmin, S. *1,3-Dienes*. Thieme: Stuttgart, 2009; Vol. 46, p 1-739.
- 23. Burks, H. E.; Kliman, L. T.; Morken, J. P. Asymmetric 1,4-Dihydroxylation of 1,3-Dienes by Catalytic Enantioselective Diboration. *J. Am. Chem. Soc.* **2009**, *131*, 9134-9135.
- 24. Satoh, M.; Nomoto, Y.; Miyaura, N.; Suzuki, A. New Convenient Approach to the Preparation of (*Z*)-Allylic Boronates via Catalytic 1,4-Hydroboration of 1,3-Dienes with Catecholborane. *Tetrahedron Lett.* **1989**, *30*, 3789-3792.
- 25. (a) Han, J. T.; Jang, W. J.; Kim, N.; Yun, J. Asymmetric Synthesis of Borylalkanes via Copper-Catalyzed Enantioselective Hydroallylation. *J. Am. Chem. Soc.* **2016**, *138*, 15146-15149. (b) Davies, S. G.; Lee, J. A.; Roberts, P. M.; Stonehouse, J. P.; Thomson, J. E. Absolute Configuration Assignment by Asymmetric Syntheses of the Homalium Alkaloids (–)-(*R*,*R*,*R*)-Hoprominol and (–)-(4'S,4"*R*,2""*R*)-Hopromalinol. *J. Org. Chem.* **2012**, *77*, 9724-9737.
- 26. Peña-López, M.; Martínez, M. M.; Sarandeses, L. A.; Sestelo, J. P. A Versatile Enantioselective Synthesis of Barrenazines. *Org. Lett.* **2010**, *12*, 852-854.
- 27. Smith, A. B.; Safonov, I. G.; Corbett, R. M. Total syntheses of (+)-zampanolide and (+)-dactylolide exploiting a unified strategy. *J. Am. Chem. Soc.* **2002**, *124*, 11102-11113.
- See Supporting Information for details.
- 29. Frisch, M. J.; Trucks, G. W.; Schlegel, H. B.; Scuseria, G. E.; Robb, M. A.; Cheeseman, J. R.; Scalmani, G.; Barone, V.; Petersson, G. A.; Nakatsuji, H.; Li, X.; Caricato, M.; Marenich, A. V.; Bloino, J.; Janesko, B. G.; Gomperts, R.; Mennucci, B.; Hratchian, H. P.; Ortiz, J. V.; Izmaylov, A. F.; Sonnenberg, J. L.; Williams-Young, D.; Ding, F.; Lipparini, F.; Egidi, F.; Goings, J.; Peng, B.; Petrone, A.; Henderson, T.; Ranasinghe, D.; Zakrzewski, V. G.; Gao, J.; Rega, N.; Zheng, G.; Liang, W.; Hada, M.; Ehara, M.; Toyota, K.; Fukuda, R.; Hasegawa, J.; Ishida, M.; Nakajima, T.; Honda, Y.; Kitao, O.; Nakai, H.; Vreven, T.; Throssell, K.; Montgomery, J. A., Jr.; Peralta, J. E.; Ogliaro, F.; Bearpark, M. J.; Heyd, J. J.; Brothers, E. N.; Kudin, K. N.; Staroverov, V. N.; Keith, T. A.; Kobayashi, R.; Normand, J.; Raghavachari, K.; Rendell, A. P.; Burant, J. C.; Iyengar, S. S.; Tomasi, J.; Cossi, M.; Millam, J. M.; Klene, M.; Adamo, C.; Cammi, R.; Ochterski, J. W.; Martin, R. L.; Morokuma, K.; Farkas, O.; Foresman, J. B.; Fox, D. J. Gaussian 16, Revision C.01; Gaussian, Inc.: Wallingford CT, 2016.
- 30. Grimme, S.; Antony, J.; Ehrlich, S.; Krieg, H. A consistent and accurate ab initio parametrization of density functional dispersion correction (DFT-D) for the 94 elements H-Pu. *J. Chem. Phys.* **2010**, *132*, 154104-1–154104-18.

- 31. (a) Fuentealba, P.; Stoll, H.; Vonszentpaly, L.; Schwerdtfeger, P.; Preuss, H. On the reliability of semi-empirical pseudopotentials simulation of Hartree-Fock and Dirac-Fock results. *J. Phys. B: At. Mol. Phys.* **1983**, *16*, L323-L328. (b) Hay, P. J.; Wadt, W. R. Abinitio effective core potentials for molecular calculations potentials for the transition-metal atoms Sc to Hg. *J. Chem. Phys.* **1985**, *82*, 270-283. (c) Andrae, D.; Haussermann, U.; Dolg, M.; Stoll, H.; Preuss, H. Energy-adjusted abinitio pseudopotentials for the 2nd and 3rd row transition-elements. *Theor. Chim. Acta* **1990**, *77*, 123-141.
- (a) Gonzalez, C.; Schlegel, H. B. An improved algorithm for reaction-path following. J. Chem. Phys. 1989, 90, 2154-2161. (b) Gonzalez, C.; Schlegel, H. B. Reaction-path following in massweighted internal coordinates. J. Phys. Chem. 1990, 94, 5523-5527. (a) Becke, A. D. Density-Functional Thermochemistry. III. The Role of Exact Exchange. J. Chem. Phys. 1993, 98, 5648-5652. (b) Hariharan, P. C.; Pople, J. A. The Influence of Polarization Functions on Molecular Orbital Hydrogenation Energies. Theor. Chim. Acta 1973, 28, 213-222. (c) Hehre, W. J.; Ditchfield, R.; Pople, J. A. Self-Consistent Molecular Orbital Methods. XII. Further Extensions of Gaussian- Type Basis Sets for Use in Molecular Orbital Studies of Organic Molecules. J. Chem. Phys. 1972, 56, 2257-2261. (d) Gordon, M. S.; Binkley, J. S.; Pople, J. A.; Pietro, W. J.; Hehre, W. J. Self-Consistent Molecular-Orbital Methods. 22. Small Split-Valence Basis Sets for Second-Row Elements. J. Am. Chem. Soc. 1982, 104, 2797-2803. (e) Francl, M. M.; Pietro, W. J.; Hehre, W. J.; Binkley, J. S.; Gordon, M. S.; DeFrees, D. J.; Pople, J. A. Self-Consistent Molecular Orbital
- 34. Marenich, A. V.; Cramer, C. J.; Truhlar, D. G. Universal Solvation Model Based on Solute Electron Density and on a Continuum Model of the Solvent Defined by the Bulk Dielectric Constant and Atomic Surface Tensions. *J. Phys. Chem. B* **2009**, *113*, 6378-6396.

Methods. XXIII. A Polarization-Type Basis Set for Second-Row

Elements. J. Chem. Phys. 1982, 77, 3654-3665.

- 35. (a) Zhao, Y.; Truhlar, D. G. The M06 Suite of Density Functionals for Main Group Thermochemistry, Thermochemical Kinetics, Noncovalent Interactions, Excited States, and Transition Elements: Two New Functionals and Systematic Testing of Four M06-Class Functionals and 12 Other Function. Theor. Chem. Acc. 2008, 120, 215-241. (b) Zhao, Y.; Truhlar, D. G. Density Functionals with Broad Applicability in Chemistry. Acc. Chem. Res. 2008, 41, 157-167. (c) Perdew, J. P.; Ruzsinszky, A.; Tao, J. M.; Staroverov, V. N.; Scuseria, G. E.; Csonka, G. I. Prescription for the design and selection of density functional approximations: More constraint satisfaction with fewer fits. J. Chem. Phys. 2005, 123, 062201-1-062201-9. (d) Tao, J. M.; Perdew, J. P.; Staroverov, V. N.; Scuseria, G. E. Climbing the density functional ladder: Nonempirical metageneralized gradient approximation designed for molecules and solids. Phys. Rev. Lett. 2003, 91, 146401-1-146401-4. (e) Staroverov, V. N.; Scuseria, G. E.; Tao, J. M.; Perdew, J. P. Comparative assessment of a new nonempirical density functional: Molecules and hydrogen-bonded complexes. J. Chem. Phys. 2003, 119, 12129-12137. (f) Weigend, F. Accurate Coulomb-fitting basis sets for H to Rn. Phys. Chem. Chem. Phys. 2006, 8, 1057-1065. (g) Weigend, F.; Ahlrichs, R. Balanced basis sets of split valence, triple zeta valence and quadruple zeta valence quality for H to Rn: Design and assessment of accuracy. Phys. Chem. Chem. Phys. 2005, 7, 3297-3305. (h) Schafer, A.; Huber, C.; Ahlrichs, R. Fully optimized contracted gaussian-basis sets of triple zeta valence quality for atoms Li to Kr. J. Chem. Phys. 1994, 100, 5829-5835. (i) Chai, J. D.; Head-Gordon, M. Long-range corrected hybrid density functionals with damped atom-atom dispersion corrections. Phys. Chem. Chem. Phys. 2008, 10, 6615-6620.
- 36. In a computational study of related reactions, that involved oxidative cyclizations of cationic Co(I)-intermediates we had explicitly considered higher spin states and ruled them out as viable intermediates based on energy considerations. Herbort, J. H.; Lalisse, R. F.; Hadad, C. M.; RajanBabu, T. V. Cationic Co(I) Catalysts for Regiodivergent Hydroalkenylation of 1,6-Enynes: An

- Uncommon cis-β-C-H Activation Leads to Z-Selective Coupling of Acrylates. *ACS Catal.* **2021**, *11*, 9605-9617.
- 37. Parsutkar, M. M.; Moore, C. E.; RajanBabu, T. V. Activator-free single-component Co(I)-catalysts for regio- and enantioselective heterodimerization and hydroacylation reactions of 1,3-dienes. New reduction procedures for synthesis of L Co(I)-complexes and comparison to in situ generated catalysts. *Dalton Trans.* **2022**, *51*, 10148-10159.
- 38. Song, L.-J.; Wang, T.; Zhang, X.; Chung, L. W.; Wu, Y.-D. A Combined DFT/IM-MS Study on the Reaction Mechanism of Cationic Ru(II)-Catalyzed Hydroboration of Alkynes. *ACS Catal.* **2017**, *7*, 1361-1368.
- 39. Liu, Y.; Jiang, Z.; Chen, J. Origin of the ligand effect in the cobalt catalyzed regioselective hydroboration of 1,3-diene. *Org. Biomol. Chem.* **2020**, *18*, 3747-3753.
- As suggested by one of the reviewers, we have conducted the hydroboration reaction in the presence of benzaldehde (also npentanal), with the hope of intercepting the Co-allyl species that accompanies the C-B or C-H bond formation in the reactions of the η<sup>4</sup>-Co-complex with aldehyde. The aldehyde had no effect on the reaction; the hydroboration products were formed in excellent yield (>80%) and enantioselectivity (er >99:1) and the aldehyde was recovered quantitatively. It is conceivable that the Co-allyl species are not nucleophilic like the Ru and Ni allvl intermediates to which this process was being compared to. Ru(0): (a) Park, B. Y.; Montgomery, T. P.; Garza, V. J.; Krische, M. J. Ruthenium Catalyzed Hydrohydroxyalkylation of Isoprene with Heteroaromatic Secondary Alcohols: Isolation and Reversible Formation of the Putative Metallacycle Intermediate. J. Am. Chem. Soc. 2013, 135, 16320-16323. Ni(0): (b) Kimura, M.; Ezoe, A.; Mori, M.; Iwata, K.; Tamaru, Y., Regio- and Stereoselective Nickel-Catalyzed Homoallylation of Aldehydes with 1,3-Dienes. J. Am. Chem. Soc. 2006, 128, 8559-8568. See Supporting Information for details (p. S42).

## **TOC Abstract**

